Low-cost Expendable UAV
Final Report

1 May 2003

Virginia Tech

Department of Aerospace and Ocean Engineering

Low-cost Expendable UAV Project

Team Lemming:

Atalla Buretta

Ryan Fowler

Matthew Germroth

Brian Hayes

Timothy Miller

Evan Neblett

Matthew Statzer

Table of Contents

List of Figures

List of Tables

Chapter 1 Introduction and Summary

The Team Lemming Cheap UAV (CUAV) design project is a response to a request for proposal from the United States Navy for a low cost, expendable UAV to be used for reconnaissance missions. The Navy would use this UAV as an alternative to more expensive manned and unmanned reconnaissance systems in situations where there is a high risk of losing the aircraft, or where extended time on station is more valuable than the recovery of the craft. For clarity, the RFP requirements are discussed below.

1.) The UAV must carry a 50 lb reconnaissance payload.

2.) The UAV must launch from a Navy ship, airplane, or helicopter.

3.) The UAV must fly for 5 hours on a predetermined circuit or accept alterations to the flight plan based on observations made by the controller.

4.) At the end of the mission the UAV will not be recovered, and will be required to crash.

In addition to the requirements set forth by the Navy, Team Lemming developed additional design specifications for our UAV concepts. These specifications are discussed below.

1.) To increase the range, adaptability, and marketability of the UAV, all concepts will be capable of aerial deployment.

2.) For agreement with the design altitude of current low cost reconnaissance cameras, the design mission altitude for the UAV shall be 5,000 ft.

3.) To allow for variations in mission profiles, a minimum service ceiling of 10,000 ft shall be required.

4.) A speed range for the UAV of 65 – 140 knots shall be required to allow deployment at a wide range of velocities.

5.) A 30 minute cruise to station shall be required in addition to the 5 hour loiter on station.

6.) Minimum climb rate of 200 fpm at 5,000 ft.

7.) Minimum climb rate of 100 fpm at 10,000 ft.

The driving factor for this design is to keep the UAV cost as low as possible while still meeting the RFP and design team requirements. The UAV acquisition cost must be low when compared to existing systems. Otherwise, the Navy will not be willing to purchase the Team Lemming UAV. As shall be noted in the performance and mission analysis chapters of this report, the Team Lemming CUAV exceeds all performance and cost specifications.

The remainder of this report documents the process followed by Team Lemming in the selection of a UAV concept for final development, and the detailed design of the final concept. The final Lemming CUAV is shown in figure 1.1. As shown in figure 1.1, the Lemming CUAV is a propeller powered craft utilizing a high wing design, and a tractor engine configuration. The wing pivots about a shaft and stores parallel to the fuselage to allow transport and launch from a variety of Navy aircraft. This wing swings open upon UAV deployment.

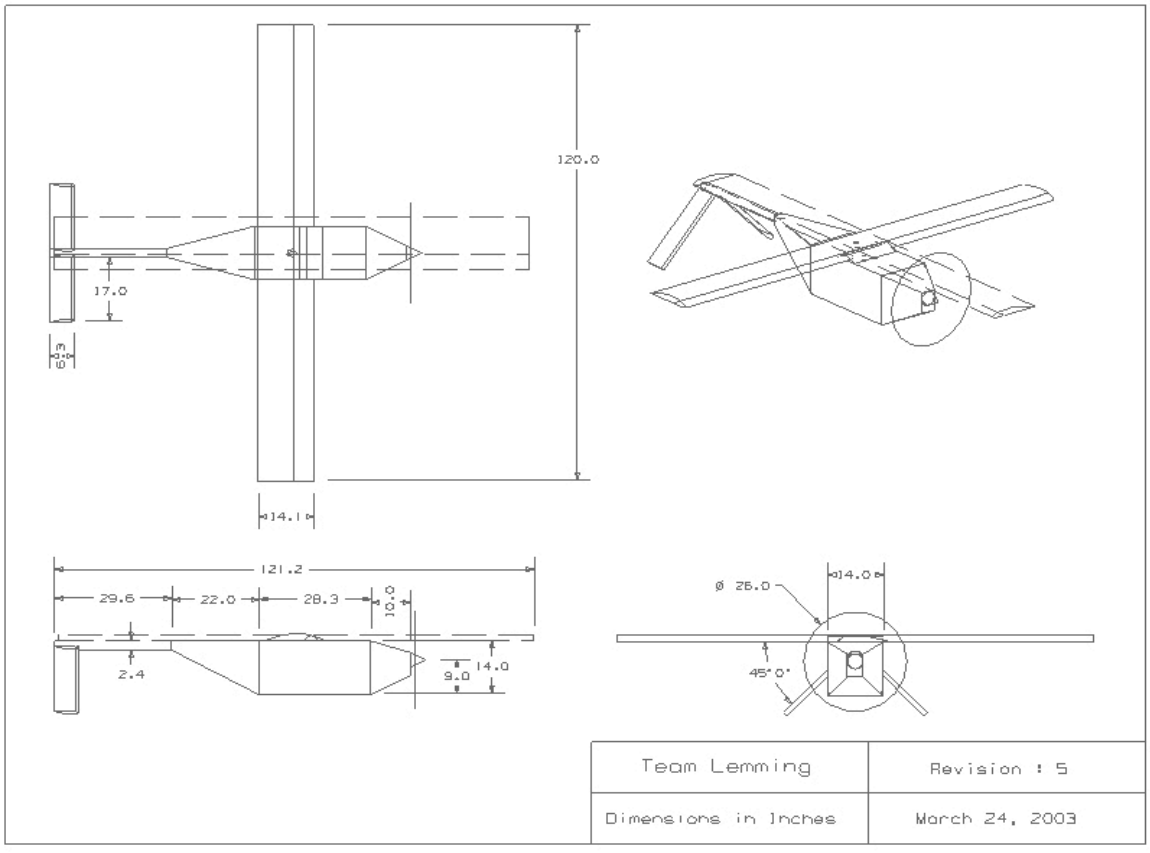

Figure 1.1: Team Lemming Cheap UAV final design.

Chapter 2 Mission Analysis and Comparative Aircraft

2.1 Mission Analysis

The RFP that the Lemming team is responding to has only one mission. This mission is a 5-hour surveillance mission at a preprogrammed circuit at a predefined altitude, or a circuit determined from observations the CUAV has made. This has left the team to define aspects such as the loiter speed and ceiling of the CUAV. The team defined a range of speeds and altitudes that the CUAV will be capable of, based on performance numbers of current UAVs.

During the Conceptual Design phase, the team decided that an aerial deployment would provide the cheapest and safest means of deploying the aircraft. This required the team to find naval aircraft that could handle the different deployment options of the team. The team scoured both the internet (References 4 and 5) and the library (References 1 through 3) to find information on current naval aircraft. Table 2.1 shows a compilation of most of the important information about the aircraft found that could deploy the CUAV. The stall speed of the transport aircraft is important because it needs to be low enough to not violate the maximum speed of the CUAV during deployment. The internal dimensions and maximum payload weight define the maximum number of CUAVs deployable from one transport, and size limitations the internal transport incurs on the CUAV. The front-line availability and life-span of the transport aircraft also weighed in the decision. In the end the C-2 was passed on as a transport option because of its ability to take off from a carrier and its higher cruise speed than other carrier launched options. The CH-53E Sea Stallion is another selected transport because of its use in Marine Expeditionary Force operations, and because it could most easily accomplish the "Towed" aerial deployment. Finally the C-130 was used because of its versatility, large cargo area, weight, range, and most importantly its long service lifetime.

Aircraft	Wpayload (lb)	W cargo hook (lb)	Width (ft)	Height (ft)	Vcr (mph)	Vso (mph)	Range (mi)	Tow Hook	Rear Door	Side Door	Hard Point	Service	Pass On
Transport													
Lockheed Martin C-130 Hercules	26534		10' 3"	9	374	115	2356		x			M	Y
Grumman C-2 Greyhound	10000		7' 4"	5' 5"	345	86	1495		x			N	Y
Bell-Boeing MV-22 Osprey	14360		5' 11"	6'	264	n/a	575	x	x			M*	Y
ASW													
Lockheed P-3 Orion	20000		6' 8"	2' 10.5"	380	154	4927				x	N	
Helicopter													
Kaman Aerospace SH-2 Super Seasprite	2693				138	n/a	518			x		NR	
Bell AH-1 Cobra	2467		10' 9"		173	n/a	322				x	M	
Bell UH-1N Huey	2000	2000			136	n/a	357	x		x		M	
Boeing CH-46 Sea Knight	4000	4000			154	n/a	151.8	x	x			M	
Sikorsky Ch-53E Sea Stallion	25000	36000	7' 6"	6' 6"	173	n/a	1139	x	x	x		N,M	
Sikorsky SH-60B Seahawk	6000				145	n/a	518			x		N,M	Y

N	Navy	NR	Naval Reserves
M	Marines	M*	Marines, Upon approval

Table 2.1 Transport Aircraft Comparatory Study

The deployment of the aircraft has a large impact on the mission of the CUAV. The team has to plan for the turbulent flows that the CUAV will be exposed to during the deployment process. In the case of the C-130 this is critical because its stall speed (100kts) is relatively high compared to the proposed maximum speed of the CUAV (120kts). In order to determine the minimum deployment speed of the C-130 the team applied a factor of safety of 1.4 to its stall speed, which is twice the traditional takeoff speed safety factor (1.2*Vso). This determined the minimum C-130 deployment speed as 140kts, which requires the team to raise the CUAV's maximum speed 20kts. When the turbulent nature of the flow is taken into account, this makes the launch segment the one that will determine the structural limits of the CUAV. Furthermore, the team is not aware of any research indicating that a UAV can be deployed using a parachute. This is something that the team will have to do further research on, which might include wind tunnel testing, or other more inventive studies.

The basic loiter mission segment doesn't impose many problems on the CUAV design, aside from the requirement that the CUAV be able to change orbit depending on observations. The team has interpreted this to mean that a human controller will provide the changes to the CUAV, instead of having the CUAV make its own orbit changes due to observations. This simplifies the onboard computer system required of the CUAV, decreasing its cost. However, it requires the CUAV to constantly stream data to

and from a remote controller station. This exposes it to being jammed by enemies, and ultimately vulnerable to being "hacked" and controlled by the enemy. The likelihood of this is slim, but it will require that the CUAV have communications gear that protects its communication. This communication requirement will add more weight and cost to the CUAV.

A final aspect of the CUAV's mission that will cause the team some trouble is the crash of the UAV. The team will have to decide whether the CUAV will carry a self-destruct system so that its technology can't be used again. This makes handling the CUAV more difficult during storage and transport. This would reduce the CUAV's storage and deployment ability, and the extra system will also increase the weight. The other option is to use the kinetic energy of the crashing aircraft to destroy its sensitive materials. This method raises concerns of making sure the CUAV will crash so that it doesn't strike a domicile, schoolhouse, or other civilian location.

2.2 Comparative Aircraft Study

A study of comparative aircraft was performed to create a historical basis for the design of Team Lemming's CUAV. This study included all forms of UAVs that might be able to accomplish the mission, including cruise missiles. Figures 2.2 and 2.3 are the compilation of UAV and Cruise Missile research respectively. This data was collected from many sources on the internet and from the library. The first list of traditional UAVs shows that there are a number of UAVs that fit all but 2 of the mission requirements; those of aerial deployment and cost. The Cruise Missiles have a more difficult time meeting the stringent RFP requirements, as their cost is high, and often their endurance times are too low. This is due, in part, to the small fuel storage space, and the use of jet engines that have higher fuel consumption rates.

An interesting thing to note is that the AAI Shadow 200 comes close to filling out the RFP requirements. It might be interesting to see if a stripped down version of the Shadow with a shorter span and no landing gear could be made to fit the RFP. However, Team Lemming believes that their CUAV design will be able to outperform this modified UAV concept. Thus, the development of the CUAV design is validated by the fact that currently no UAV exists that fills all the RFP requirements.

Table 2.2: Comparative Aircraft - Traditional UAVs

Name	AAI Pioneer	AeroVironment Sass Lite	AAI Shadow 200	AAI Shadow 400	DRS Unmanned Technologies "Sentry"	Freewing Scorpion 100-50	Westing house Huntair	BAI Aerosys. Porter	D P Assc. Truck
Payload (lb)	100	100	55.7	66	75	50	80	75	50
Endurance (hr)	5.5	5	5.0 - 6.0	5	8	3.5	7.5	4	4
Span, b (ft)	16.9	n/a	12.75	16.8	11	16.1	11.7	20	12.7
Length, l (ft)	14	63	11.17	12.54	7.96	11.8	7.5	12	9.7
Height, lh (ft)	3.3	21							
W_{GTOW} (lb)	450	800	327	442	250	475			
Power, P (hp)	26		37		25.5	65	38	22	17
Max Speed, Vmax (mph)	115	40	141.5	115	115	172	150	80	
Cruise Speed, Vcr (mph)	92	15	96.67	86		75	115	50	121
Loiter Speed, Vlt (mph)			74.8	74.8		69			
Range (mi)	115	75	580.02	430	230	260	31	30	794
Max Altitude (ft)	15000	9850	15000	12000	16000	15000	17000	5000	5000
A/C Price ($100,000)			0.5						0.35
Droppable	N	N	N	N	N	N	N	N	N
	Range limited by 185km jam-resistant data link	Derrigible			Delta Wing... raised hor tail, two booms to twin Vert tails	*6.5 hr endurance is at 31 mi range			

Table 2.3: Comparative Aircraft - Cruise Missiles

Name	AGM-158 JASSM	AGM -137 TSSAM	AGM-154 JSOW	AGM-142 Raptor	AGM-136 Tacit Rainbow	BGM-109 Tomahawk	AGM-86C CALCM	AGM-86B CALCM
Payload (lb)		1000	1000	770	40	1000	1500	Nuclear, W-80-1
Endurance (hr)	0.5					1.26		2.73
Span, b (ft)		8.3		6.5	5.167	8.75	12	12
Length, l (ft)		14	13	15.83	8.33	18.25	20.75	20.75
Height, lh (ft)				1.75		1.7	2.05	2.05
We (lb)							250?	1500
W_{GTOW} (lb)		2000	1500	3000	430	2650	3250	3150
Engine	small turbojet			solid prop. Rocket	Williams Int. F121	Will. Int. F107-WR-402	Will. Int. F-107-WR-101	Will. Int. F-107-WR-101
Power, P (hp)					70 lbs	600lb	600lb	600lb
Cruise Speed, Vcr (mph)					Subsonic	550	High Subsonic	550
Range (mi)		115	138	57.5	267*	690	690	1500+
A/C Price ($100,000)	7	20.62	2.82 - 7.19	15.4	2	5.75 - 14	6.0 - 18	1.0 - 10
Deployable	Y	Y	Y	Y	N	N	Y	Y
Notes		killed after cost climbed from $728,000			*ground launched. 50+mi air-launched	aluminum, *block III; G model range of 1300mi on -440 engine	AGM-86D Block II flew for 4.5 hours	1360 fuel weight based on weight of BGM-109

Chapter 3 Deployment

The method of the low-cost, expendable UAV's deployment was initially considered due to the strong dependence of the UAV's design on the deployment method. Eight deployment options were

considered. These options were divided into two groups: aerial deployment and surface deployment. To minimize the cost of the UAV and improve mission and location versatility, the traditional take-off method was not considered. The landing gear required for traditional take-off greatly increases the cost, weight, and complexity of the UAV design. In addition, a runway is needed in a controlled location, greatly reducing the reconnaissance capabilities of the aircraft.

The aerial deployment options involve the use of an airplane or helicopter to transport the UAV to the specified drop zone. The surface deployment options involve a launch from a ship or submarine. It was decided for the purposes of versatility and marketability that the UAV would be designed for compatibility with three aerial deployment options.

3.1 Aerial Deployment

Within the aerial deployment category, five options were analyzed. The five aerial deployment options considered were the simple drop, parachute assisted drop, boom launch, hard point launch, and tow line. An initial bias was given to the aerial deployment options due to the immensely greater positioning versatility they exhibit when compared against the surface deployment options. The following is a summary of the aerial deployment options.

3.1.1 Simple Drop

The simple drop method is the simplest aerial deployment method, and involves pushing the plane out of the rear cargo door of the transport aircraft. The UAV is expected to fall a predetermined distance and then pull out of the dive once it has gained control. The main advantages to this deployment option are its low cost and the fact that it would require minimal modifications to both the UAV and the transport aircraft. The disadvantages to this option are the UAV size restrictions stemming from the internal storage and the stability and control issues associated with the dive recovery.

3.1.2 Parachute-Assisted Drop

The parachute-assisted drop is much like the simple drop, save for a parachute attached to the tail section of the UAV. The parachute would be used as a drag chute to pull the UAV out of the back of the transport aircraft, and then to control the descent velocity and provide stability during deployment of

flight surfaces. After the deployment of flight surfaces and engine start-up, the UAV would be released from the chute. The advantages to this option are its simplicity and inherent stability provided by the chute. The disadvantages to this deployment option are the size restrictions imposed on the UAV and the discarding of the drag chute after launch.

3.1.3 Boom Launch

The boom launch option involves the mounting of the UAV to a boom that extends from the transport aircraft. The boom is used to position the UAV behind the transport aircraft prior to release. The primary advantage to this option is the simplicity in release due to the pre-launch positioning of the craft in its autonomous flight position. The disadvantages to this option are the inherent cost of the boom design and the internal storage size restrictions imposed on the UAV.

3.1.4 Hard Point Launch

The hard point launch option involves the mounting of the UAV to a hard point on the transport aircraft and then releasing it. The UAV would be released from the transport aircraft and then enter sustain flight on its own. The advantages to this option are the minimal modifications required for the transport aircraft and the method's proven history. The disadvantages to this option are that the external storage of the UAV would require a stronger structure to withstand the cruise speed of the transport and the store/separation issues associated with a deployment so far forward on the transport craft.

3.1.5 Tow Line

The tow line involves pulling the UAV behind a helicopter. The UAV would be towed to its deployment location and then released from the helicopter. The advantages to this deployment option are its low cost, the lack of UAV size restrictions, and the fact that the transport cruise speed is near that of the UAV. The disadvantages to this option are that it is limited to helicopter transportation to prevent exceeding the UAV max speed, and the fact that only one UAV launch is possible per transport.

3.2 Surface Deployment

Three surface deployment options were considered: the ship rocket-assisted take-off (RATO) launch, the submarine launch, and the ship catapult launch. With surface deployment, the transportation of the UAV to its launch site would never require the aircraft to endure strenuous speeds, as is the case with the externally stored aerial deployment options.

3.2.1 Ship RATO Launch

The RATO launch from the deck of a ship would be executed by placing a small rocket on the underside of the UAV, used to accelerate the UAV to its cruise speed and position. The advantages to this option are the lack of size restrictions on the UAV and multiple UAV launch capability. The disadvantages to this option are that the launch would be limited to coastal regions and the increase in structural design costs due to the high launch velocity.

3.2.2 Submarine Launch

The submarine launch option is similar to the ship RATO launch, except for the fact that the UAV is first launched from the submarine in an ICBM tube before the rocket is fired above the surface of the water. The primary advantage to this design is the stealth of the transport submarine. The disadvantages to this deployment option are its cost ineffectiveness and the fact that the deployment is limited to coastal regions.

3.2.3 Catapult Launch

The catapult launch option involves mounting a catapult to a ship, and then launching the UAV with sufficient velocity for the aircraft to sustain flight autonomously. The advantages to this deployment option are that it is a proven launch method, multiple UAV deployment capability, and its cost effectiveness. The disadvantages to this option are that deployment is limited to coastal regions and calm seas would be required for a catapult launch.

3.3 Selection of Deployment Options

In the selection of the deployment options, a decision matrix was constructed based on six factors of merit (FOM). The factors of merit were quantified with a one through five weighting scale, respectively low to high importance. The first factor of merit was the effect that the particular option has

on the UAV cost, and was given a weight of five due to its high correlation with the project objective. The second factor of merit was the deployment system cost, with a weight of three. The third factor, given a weighting of four, was the feasibility of the deployment option. The feasibility FOM was based on the existence, or lack thereof, of similar technology. The reliability of the deployment option was the fourth FOM, given a rating of two. The fifth FOM, the safety of the deployment option, was also given a factor rating of two due to the expendability project requirement. The final FOM was the UAV launch quantity capability of the deployment option, and was given a one in weighting, because the RFP is for reconnaissance, which is generally done by a single UAV or aircraft. From these factors of merit, the decision matrix shown in Table 3.1 was constructed.

Table 3.1: Decisions matrix for UAV deployment options.

	FOM	UAV Cost	System Cost	Feasability	Reliability	Safety	# Deployed	**Totals**
	Ranking	5	3	4	2	2	1	
Deployment Options								
Hard Mount - Helo		2	4	5	4	3	2	58
Hard Mount - A/C		1	4	5	4	2	3	52
Tow Line Helo		4	5	5	3	4	1	70
Internal - Boom Deploy		5	2	3	3	4	4	61
Internal - Parachute Deploy		5	4	5	4	4	5	78
Internal - Simple Drop		5	4	4	4	3	5	72
Ship Launch - RATO		1	2	4	3	2	5	42
Ship Launch - Catapult		2	2	4	4	3	5	51
Sub Launch - RATO		1	1	2	4	2	2	30

The decision matrix shown highlights the highest scoring deployment options. The orange highlighted option is the simple drop. The simple drop method, originally considered viable, was discarded because the team wasn't sure the UAV could recover itself. Therefore, the three options highlighted in yellow are the three deployment options selected. Diagrams of the three selected deployment options are shown in Figures 3.1 – 3.3.

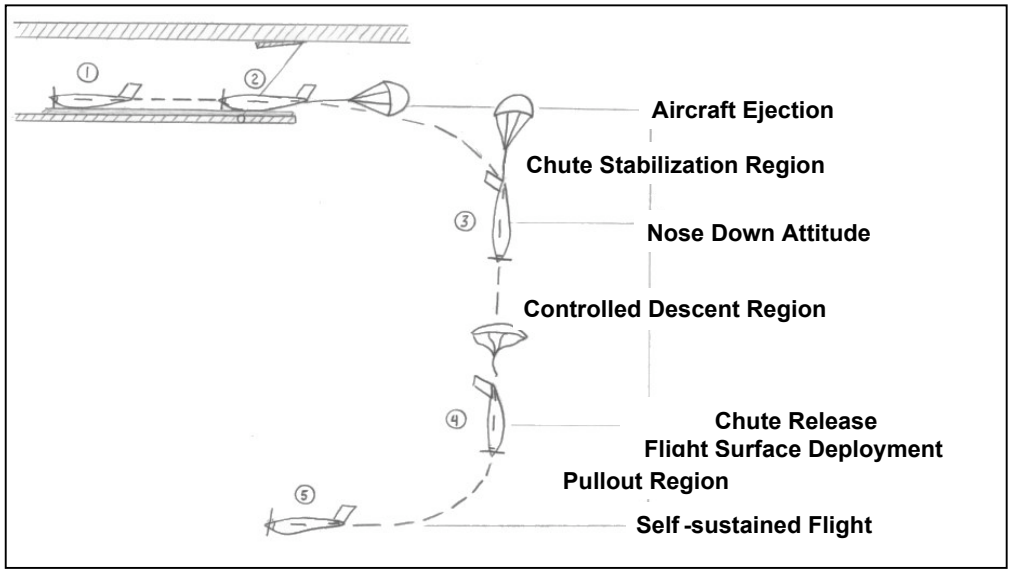

Figure 3.1: Schematic of parachute assisted launch method

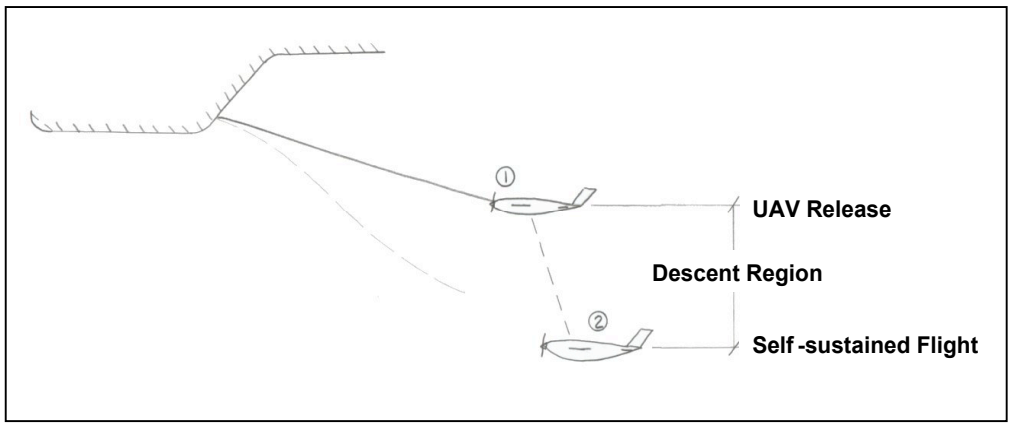

Figure 3.2: Schematic of helicopter tow-line launch method

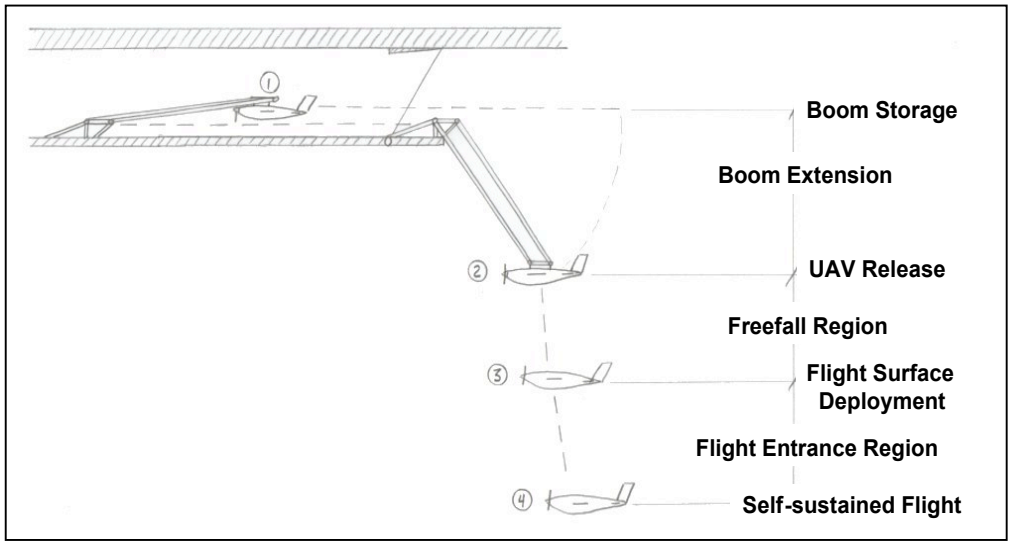

Figure 3.3: Schematic of boom assisted launch method.

Chapter 4 Selection of a Preferred Design

4.1 Preliminary Concepts

Each member of Team Lemming created a UAV configuration concept as a solution to the CUAV RFP. From these original concepts, five distinct designs were produced. The original concepts are as follows: a conventional concept with folding wings, a delta wing concept, a scissor wing concept, a canard concept, and a rotary wing concept. A graphical summary of the initial concepts and the selection process is shown in figure 4.1.

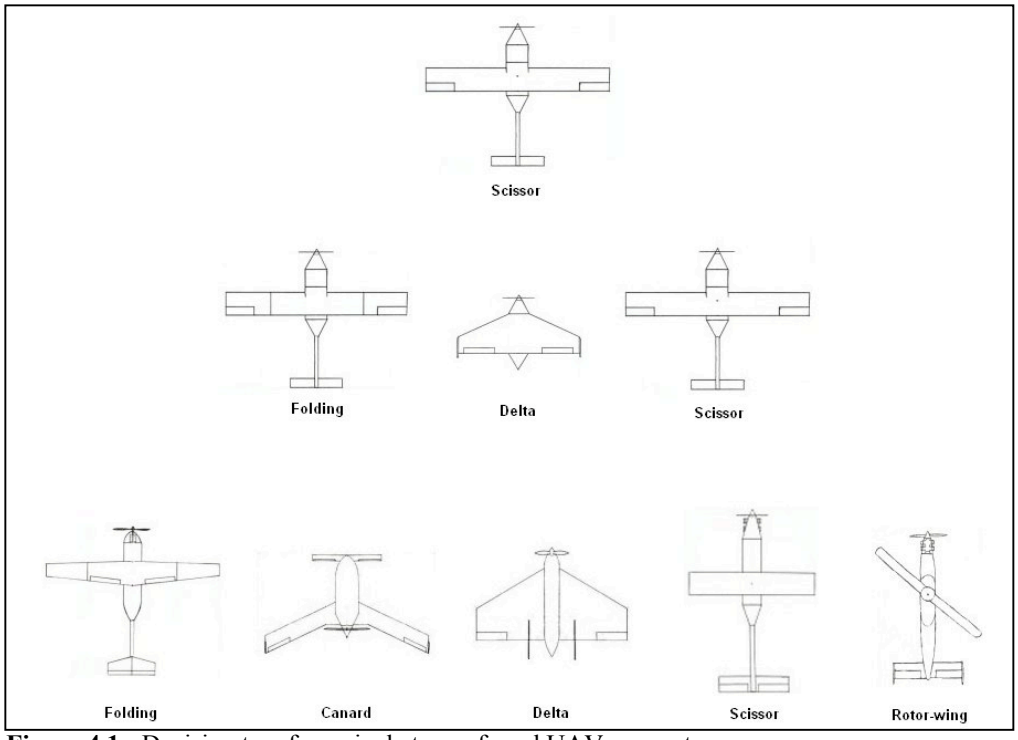

Figure 4.1: Decision tree for arrival at a preferred UAV concept.

4.2 Pro & Con Analysis

Each concept was analyzed to determine its advantages and disadvantages as related to the RFP. Factors of merit were developed to quantitatively rank the suitability of the concepts to the CUAV project, and ultimately determine three preferred concepts to be considered for further development. Detailed analysis of the three intermediate concepts yielded a final preferred concept configuration.

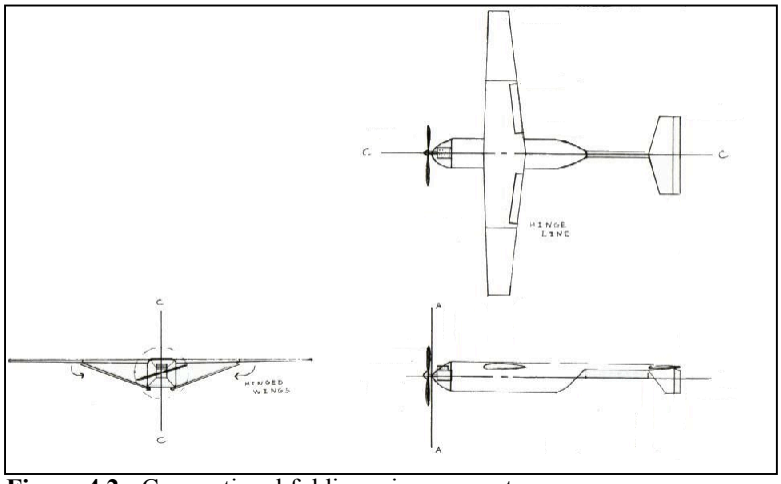

Figure 4.2: Conventional folding wing concept.

The first concept (figure 4.2), the conventional concept with folding wings, resembles a standard aircraft. It has one large, fixed wing near the front of the plane with vertical and horizontal surfaces in the rear of the plane. The design, however, would include folding wings to allow the aircraft to fit into the transport aircraft. The advantage to this design is that allows standard parts to be utilized, reducing costs of design and production. The difficulty in this design is that a folding wing is required for the aircraft to fit into the small spaces in transport aircraft. Having these folding wings unfold during flight provides an interesting dynamics problem that would increase the cost of the aircraft through structural reinforcement and damping devices.

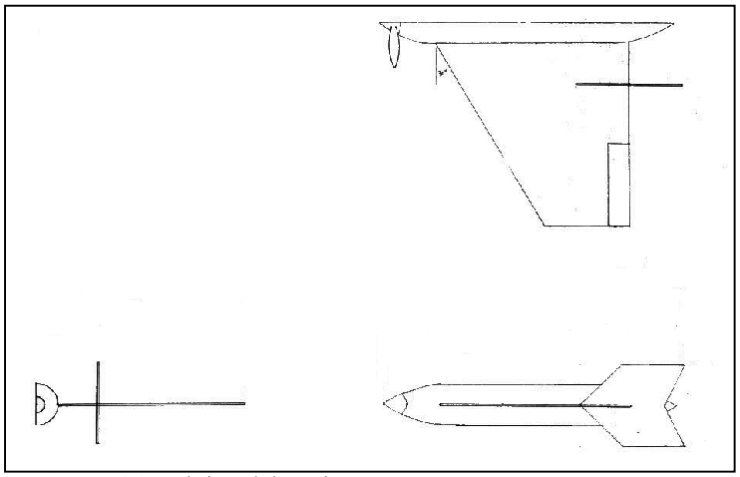

Figure 4.3: Flying delta wing concept.

The second concept analyzed was the delta wing concept (figure 4.3). This design has one large, fixed wing with vertical surfaces on the tips and no other horizontal surfaces. This allows the fuselage of the aircraft to be much shorter. The one horizontal surface has a larger mean chord than the other designs

and a shorter wingspan that allows the aircraft to fit in transport aircraft without having the wings fold. However, this wing also provides less aerodynamic efficiency, specifically in drag. Also, due to the flying wing design of this concept, the center of gravity must be carefully placed or the aircraft will become unstable in flight.

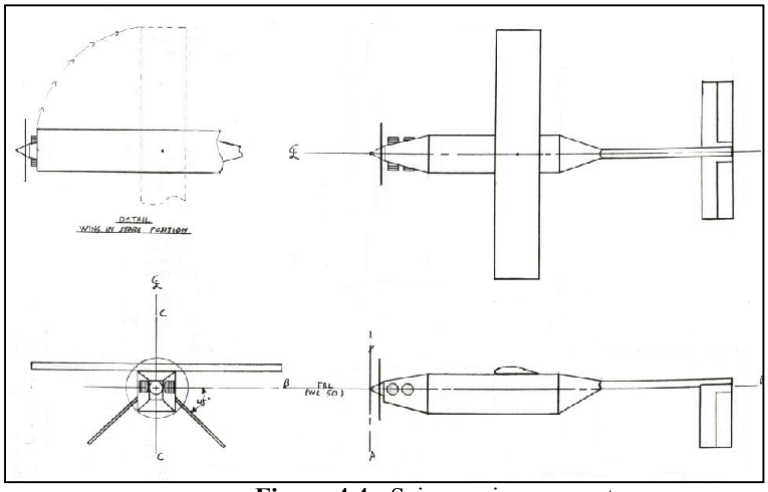

Figure 4.4: Scissor wing concept.

The scissor wing concept (figure 4.4) is similar to the conventional/folding wing concept mentioned earlier. The shape is once again similar to the standard aircraft with one large wing in the front and vertical and horizontal surfaces in the rear. As with the conventional/folding wing concept, standard parts can be utilized to save costs in design and production. Instead of having the wings fold to fit into the transport aircraft, the entire wing turns on a swivel allowing wing storage parallel to the fuselage. This design allows the wing to swing back into place at launch. Unlike a normal scissor wing, the swivel design has one side of the wing pushing through the air and the other side being pulled through the air. The forces should balance each other out, meaning less effort is needed to move the wing into position. However, to reduce the moment of inertia of the wing and avoid rotation of fuel lines, the fuel will be stored in the fuselage.

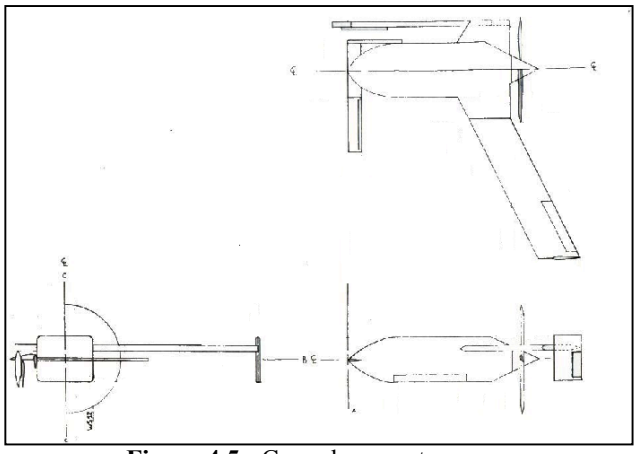

Figure 4.5: Canard concept.

The fourth concept analyzed is a canard concept (figure 4.5), with a large, fixed wing and a vertical surface in the rear and a smaller horizontal canard in the front. This configuration gives the aircraft the potential for stall control aerodynamics, and increases the aerodynamic efficiency by not requiring the airplane to fly in its own prop-wash. However, the center of gravity must be carefully placed or the aircraft could become unstable. Also, the large wing in the back must fold for internal storage in the transport aircraft. Once again, the folding wing device increases the cost of the aircraft.

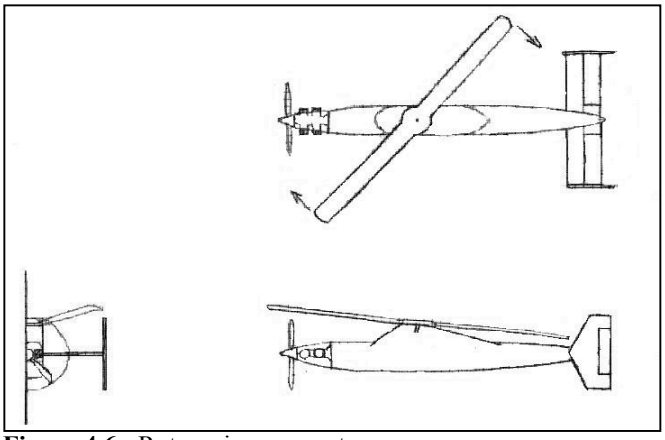

Figure 4.6: Rotor wing concept.

The fifth design concept is a rotary wing aircraft (figure 4.6). This design offers the unique ability to be able to hover almost stationary of at very slow speeds. The compactness of this design provides easy storage in the transport aircraft, but its complexity will increase the cost of the aircraft significantly.

4.3 Preferred Concept Selection

To narrow down the five unique concepts discussed above, an accurate quantitative comparison method was derived. The five concepts were judged on five parameters. These five factors of merit (FOMs) were; deployment feasibility, design complexity, lift over drag ratio, stability and control, and durability

The relevance of the different FOMs to the mission RFP was then quantified using an adaptive weighting system. This was done to ensure that the judgment parameters most important to the team mission were also the most important in the UAV concept selection process. Each FOM was ranked from 1 to 5, with 1 representing the lowest design priority and 5 representing the most important FOM.

Once the five FOMs and weighting system had been formulated, the concepts could be judged and compared. Keeping in mind the function of the aforementioned method was to narrow down the number of UAV concepts to be considered, the comparison was achieved with educated estimates. Each concept was given a score from 1 to 5 (low to high) for each of the five FOMs. After the scores were assigned, each one was multiplied by the corresponding FOM weight. Then the weighted scores were summed for each concept, providing a total score. Table 4.1 shows this scoring system in tabular form.

Table 4.1: Initial UAV selection matrix.

FOM		Deployment	Complexity	L/D	Stab & Cont	Durability	Totals
Ranking		4	5	3	2	2	
UAV Concepts							
Conventional		2	4	4	4	3	54
Delta		4	4	3	2	4	57
Canard		2	3	4	2	3	45
Scissor		5	3	4	4	3	61
Rotor		3	2	3	4	2	43

In Table 4.1, the 3 highest scoring initial concepts are highlighted in yellow. As shown in the table, the three concepts chosen for further analysis were the conventional, delta wing, and scissor wing concept. A detailed analysis of these concepts in presented in the following section.

4.4 Detailed Analysis Procedure

For purposes of initial sizing and performance evaluation, the folding wing and scissor wing concepts were treated as the same aircraft. The assumption was made that differences in gross weight and

performance between the two size altering techniques would be minimal. Furthermore, the folding wing concept was adjusted to include an inverted V-tail similar to the scissor wing concept. This change was done to take advantage of cost and weight savings resulting from the construction of only two control surfaces and the applicability of a the V-tail to full-flying control surfaces.

Since the folding wind and scissor wing concepts were treated as the same aircraft for sizing and performance calculations, sizing and performance analysis can only differentiate between the delta wing and the conventional winged concept. Additional analysis to determine the preferred method of varying wing geometry will be presented later in the chapter.

4.5 Initial Sizing

Initial sizing of the UAV concepts chosen for further development was based on historical data. The data from the comparative aircraft study (see chapter 2) was used to estimate the takeoff gross weight (TOGW) of the three concepts. Using the comparative aircraft study as guide, it was found that the weight build up equation for composite construction, homebuilt aircraft given by Daniel Raymer [4.1] could accurately describe reconnaissance UAVs. The equation gives the empty weight fraction as a function of W_O, AR, Hp/W_O, W_O/S, and V_{max}. The weight fraction equation is given in equation 4.1.

$$W_e/W_o = 0.69W_o^{-0.1}AR^{0.05}Hp/Wo^{0.1}W/S^{-0.05}Vmax^{0.17} \qquad \textbf{EQN 4.1}$$

In addition to the weight fraction equation, it was also necessary to estimate the mission fuel fraction of each UAV concept. Analysis of this step was performed under the assumption that the Cheap UAV only has two mission segments. That is, the craft is designed to launch from the parent craft and cruise to the target area for up to 30 minutes. Once over the target, the UAV will loiter for a period of 5 hours. As the UAV will be optimized for loiter, it was assumed that the cruise speed will be the same as the loiter speed. Therefore, in computation of fuel fraction, only the endurance fuel fraction equation was used with a total endurance time of 5.5 hours. The endurance fuel fraction equation is given in equation 4.2.

$$W_i / W_{I-1} = \exp(-EVC/\_P(L/D)) \qquad \textbf{EQN 4.2}$$

Where E = endurance time, C = specific fuel consumption, and L/D is the lift to drag ratio for loitering. A design loiter velocity of 135 ft/s and a propeller efficiency $\eta_P = 0.8$ were assumed for the both concepts. The sfc for a propeller plane is given by equation 4.3.

$$C = C_{bhp} V / [550 \eta_P] \qquad \textbf{EQN 4.3}$$

From Raymer, table 3.4 the C_{bhp} for a fixed pitch-piston prop is 0.5. Plugging these values into equation 4, yields: C = 0.1534 1/hrs.

Using figures 3.5 and 3.6 from Raymer, the loiter L/D for the conventional UAVs was estimated to be 14, while the loiter L/D for the Delta wing was estimated to be 11. Plugging these numbers into equation 3 resulted in a loiter fuel fraction of 0.9415 for the conventional concepts, and 0.9415 for the delta wing concept.

The fuel fraction Wf/Wo is given by equation 4.4

$$Wf/Wo = (1-W1/Wo) \qquad \textbf{EQN 4.4}$$

Using the above numbers in equation 4.4, a total fuel fraction for the conventional UAVs was found to be 0.0585, while the flying delta wing had a total fuel fraction of 0.0738.

A Matlab script based on equation 4.1 and incorporating the fuel fraction estimates was written to estimate the TOGW of the concepts. In the program, a design CL of 0.8 was assumed. A 9 Hp engine was assumed to power both concepts. The aspect ratio of the conventional concept was set to be 8, and the span of the delta wing concept was set to 7 ft. The program began with a rough guess of 200 lb for the TOGW and integrated using equation 4.1 and the fuel fraction equations to determine a TOGW. Results from the sizing program are shown in Table 4.2.

Table 4.2: Results of Matlab sizing code.

	Conventional	Delta
Weight (lbs)	187.00	193.00
Span (ft)	10.00	7.00
Planform Area (ft^2)	12.52	12.92
W / S	14.94	14.94
AR	8.00	3.83

It should be noted that the results of the sizing program were verified by a second Matlab script utilizing a less detailed sizing method based on equations from Raymer. Furthermore, additional confirmation of the sizing results was performed using the program Acsize[4.2], which is based on the Nicolei sizing method. Results from these sizing methods showed differences between the calculated values of less than 5 %. Please see reference 4.3 for a more detailed discussion of these results.

4.6 Tail Area Calculations

The size of the concepts' tails was required for estimation of the drag of the concepts, as well as to find out if the tail size would violate any of the size constraints of the transport aircraft. The team used Raymer's [4.1] historical data for the horizontal and vertical tail volume coefficient. The factors for homebuilt aircraft were used because the CUAV closely resembles a homebuilt aircraft in terms of size and performance, and is also not constrained by the FAR regulations, which would apply to other general aviation aircraft.

The delta wing concept only has vertical tails to size. Instead of a separate horizontal tail the delta concept will use a combination Elevator and Aileron (Elevon) on the TE of its wing. The tails were planned on being placed at the tips of the wings so that they would be easier to mount. Placing the vertical tails here would also have an end-plate effect, improving the efficiency of the wing. A simplification that the quarter chord of the vertical tail would be placed at the quarter chord of the wing tip was used to speed the calculation of this area. This resulted in a tail length of 0.7118ft.

$$S_{VT} = \frac{C_{VT} b_W S_W}{L_{VT}} \qquad \textbf{EQN 4.5}$$

The delta wing was found to require a total of 5ft^2 using Raymer's formula for vertical tail volume coefficient, equation 4.5. This area would be split between two different tails. This formed into a delta wing tail that would extend above and below the wing, minimizing the height of the aircraft. A delta wing form for the tail was used to place the rudder control behind the wing, so that the wing would not have to be notched to allow for deflection of the rudder. This would also allow a longer elevon length, which would improve the longitudinal stability of the concept.

The conventional and scissor wing concept both utilized an inverted V tail planform. The tail length was defined as half the span distance from the quarter chord location on the fuselage. This was chosen in order to minimize the aircraft length, while still protecting the rearward part of the wing during storage and transport. Both vertical and horizontal tail areas were computed using equation 4.5, and Raymer's formula for horizontal tail volume coefficient is given by equation 4.6:

$$S_{HT} = \frac{C_{HT} C_W S_W}{L_{HT}} \qquad \textbf{EQN 4.6}$$

These computations resulted in a required horizontal tail area of 1.564ft^2, and a required vertical tail area of 1.0ft^2. This showed that the horizontal tail area was the driving area in determining the tail size. The "V-tailed" configuration necessitated that the V still retain the required planform of area computed using Raymer's equation. Thus, a basic horizontal tail layout was produced having a length of 3.128ft, and a chord of 0.5ft. To come up with the actual tail length (length from the boom, along the tail, to the tip) an anhedral angle of 45º was used, resulting in an actual tail length of 2.21ft.

4.7 Concept Drawings

With the wing sizing produced from the sizing codes and the calculation of tail sizing performed in section 5.4, the concepts can now be redraw to accurate dimensions. Figures 4.7 – 4.9 are the sized and dimensioned concepts as determined by the sizing analysis.

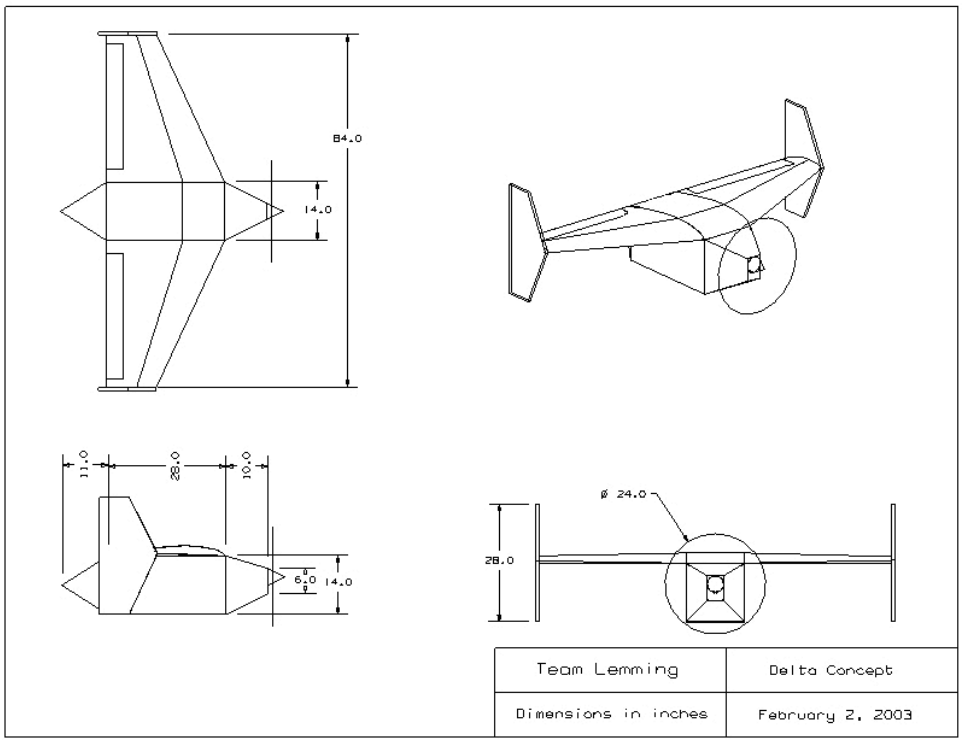

Figure 4.7: Dimensioned drawing of Delta Wing design.

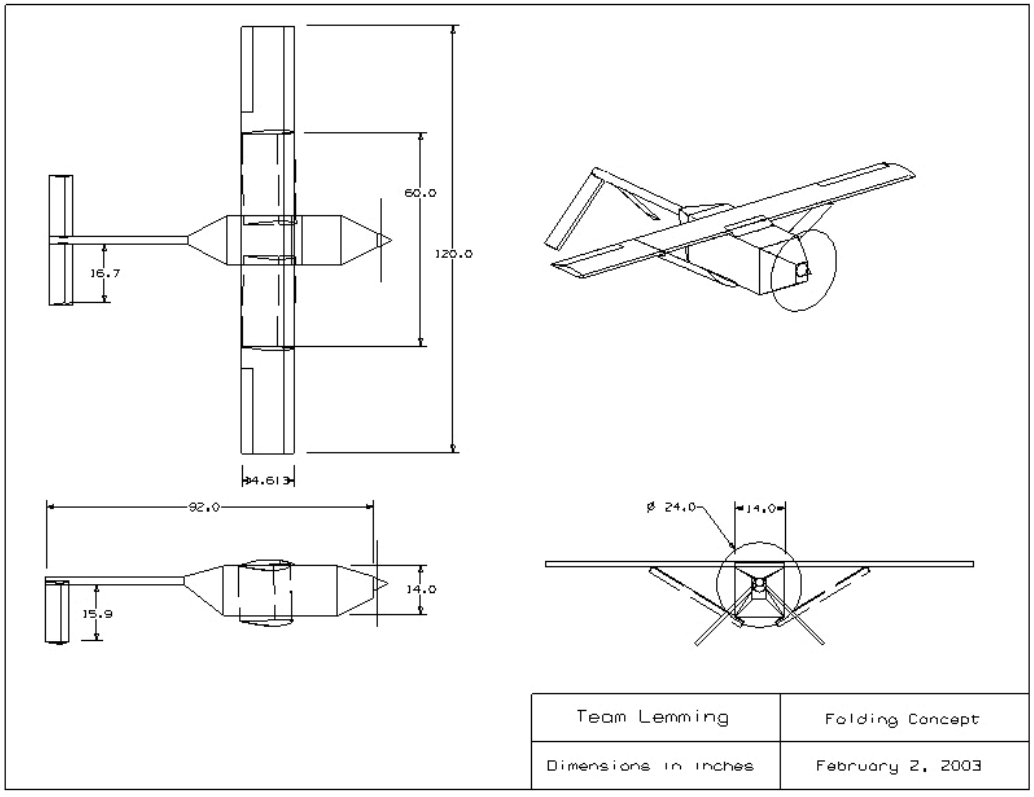

Figure 4.8: Dimensioned drawing of Folding Wing design.

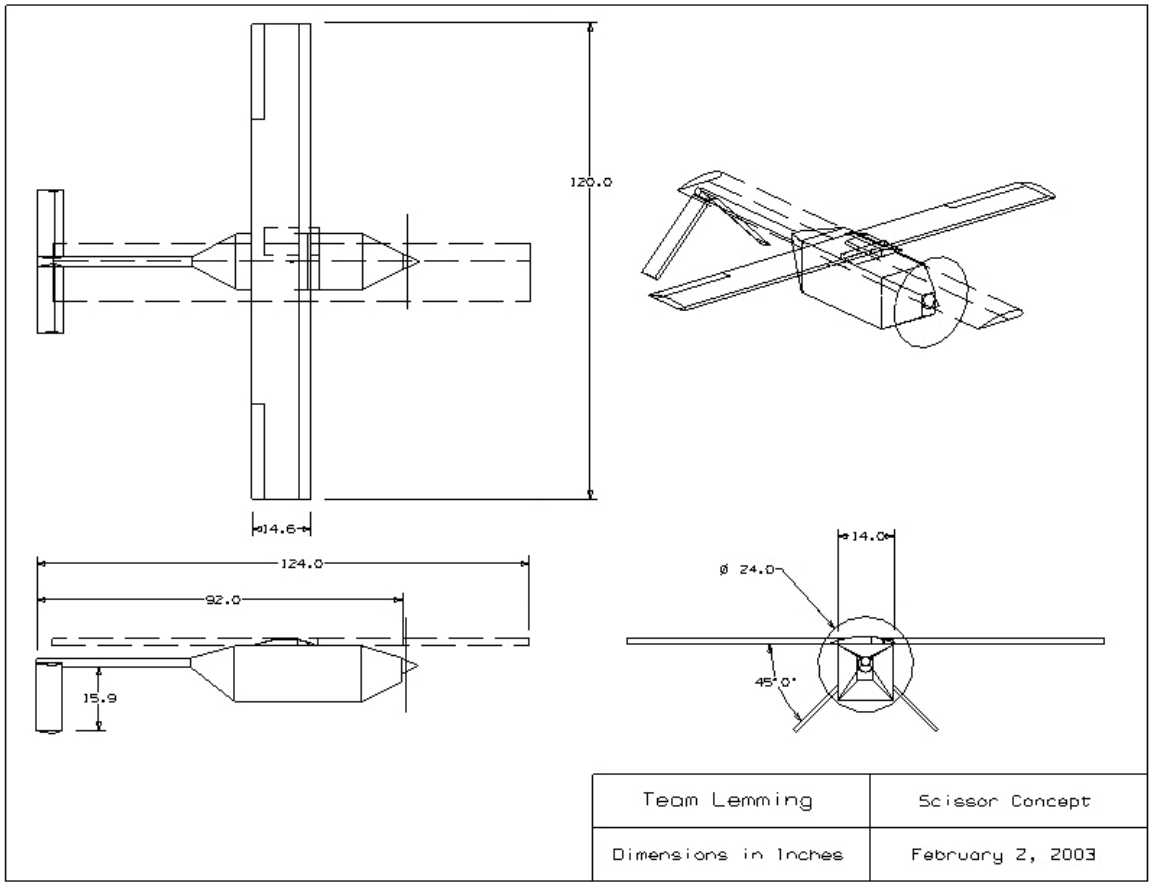

Figure 4.9: Dimensioned drawing of Swing Wing design.

4.8 Drag Calculation

To determine the power requirements of the concepts, the drag due to form and friction needed to be estimated. The program "Friction," [4.4] available in the Aircraft Design Software bundle, was used to find these values. Three different flight regimes were investigated representing the maximum speed at loiter altitude, the loiter flight regime, and loiter speed at maximum ceiling. This corresponded to 1) Altitude = 5kft, V = 140kts; 2) Altitude = 5kft, V = 80kts; 3) Altitude = 10kft, V = 80kts. The wetted area of concepts was found using the concept drawings and the simplification that a wing wetted area was twice the wing area. The wetted area of the delta wing's payload area (box cross-section portion) of the fuselage was calculated on three sides, since the third side would be covered entirely by the wing. The delta wing was found to have 50.687ft^2 of wetted area, while the conventional and scissor wing concepts had 52.46ft^2 of wetted area. The fuselages were assumed to be turbulent, while wings were given a forced transition at 0.3% of the chord, which the location of maximum thickness on 4 digit series airfoils.

This was done because the tractor propeller would make the flow around the fuselages turbulent. The forced transition of the wings was done to estimate the amount of laminar flow that the wings might reach. Mach number and altitude definition of the flight condition were used on the input files. Table 4.3 gives the results from the friction program, as well as a calculation of the total drag of the concepts at the 3 flight conditions.

Table 4.2 also holds the validation data, which was taken from the 2001-2002 VT DBF airplane. The top speed of this aircraft was found to be 47mph, based on calculations of the time the aircraft took to fly a lap at competition, and an estimated lap length. The team had access to propulsion data taken by Dzelal Mujezinovic in the Virginia Tech Open Jet Wind Tunnel. This data showed that the Astro Cobalt 60 motor with a 22x12 propeller had 1.5lbs of thrust at 47mph. As can be seen from Table 5.8 this shows that the Friction program over estimated the drag by 0.3lbs. This is only a 20% error in the drag calculation, which is acceptable during the preliminary estimation of the concepts. The error also makes the drag calculation of the concepts conservative, which will make the performance requirements more conservative. This means that as further optimization of the final design is conducted the weight and drag of the aircraft will diminish.

Table 4.3: Drag Estimation and Validation

	Delta	Conventional	DBF 1
Cdo Case1	0.0158	0.0160	0.0151
Cdo Case2	0.0177	0.0181	
Cdo Case3	0.0182	0.0186	
C_L Case1	0.2649	0.2707	0.6439
C_L Case2	0.8115	0.8036	
C_L Case3	0.9441	0.9349	
Cdi Case1	0.0058	0.0029	0.0156
Cdi Case2	0.0547	0.0257	
Cdi Case3	0.0741	0.0348	
Cd Case1	0.0216	0.0189	0.0307
Cd Case2	0.0725	0.0437	
Cd Case3	0.0923	0.0533	
D Case1	15.7250	13.7831	1.8503
D Case2	17.2334	10.4034	
D Case3	18.8686	10.9033	
case1: V = 140kts, h = 5kft			
case2: V = 80kts, h = 5kft			
case3: V = 80kts, h = 10kft			

4.9 Engine Requirements

Because the CUAV is an un-manned vehicle, it is exempt from MIL and FAR flight performance specifications. Consequently, Team Lemming developed its own performance requirements for the CUAV concepts. The team performance specifications were based on level flight performance and climb requirements. These performance requirements consequently determined the engine power needed for each concept.

For level flight performance, the team specified that the CUAV must be able to maintain the design loiter velocity of 135 ft/s at all altitudes, including the 10,000 ft service ceiling. For climb requirements, the team considered variations in the mission the CUAV might be required to perform. Although the design altitude for the CUAV is 5,000 ft, it is conceivable that for purposes of radar avoidance the Navy would desire to deploy the CUAV at essentially zero altitude. From this launch altitude the CUAV would be required to climb to the reconnaissance altitude of 5,000 ft. Team Lemming determined that the CUAV should be able to climb from sea level to 5,000 within the 30 minute cruise

time to station. This corresponds to an average climb rate of 167 ft/min. This value was rounded up to 200 ft/min climb, with the stipulation that the CUAV be able to maintain this rate of climb at 5,000 ft. The second climb requirement set forth by the team is that the CUAV be able to achieve a 100 ft/min climb rate at the service ceiling of 10,000 ft.

From the above stated performance requirements and drag calculations, it was possible to determine the engine power required by each concept to fulfill the performance requirements. Power required was determined by equations 4.7 and 4.8, which were taken from Raymer [4.1] .

$$Hp = T\ V/(550\ \eta_P) \qquad \textbf{EQN 4.7}$$

$$T = (D/W + G)\ W \qquad \textbf{EQN 4.8}$$

In Equations 4.7 & 4.8, propeller efficiency η_p was assumed to be 0.8. Furthermore, the Hp value resulting from Eqn 4.7 was divided by the density ratio at altitude to determine the altitude corrected Hp. The results of the engine power study are shown in Table 4.4.

Table 4.4: Concept engine requirements in sea-level horsepower

Altitude Corrected Horsepower Required		
	Delta	Conventional
Cruise 5,000 ft, 80 knots	7.29	4.21
Cruise 5,000 ft, 140 knots	10.46	8.9
Cruise 10,000 ft, 80 knots	9.39	5.21
100 fpm climb at 10 K ft	10.38	6.17
200 fpm climb at 5 K ft	8.98	5.85

4.10 Variable Geometry Analysis

In the UAV concept selection process, a detailed analysis of the "folding wing" concept was performed to access the merits of this concept. Two styles of folding wings were examined; the "fold-down" and the "fold-up" design (see Figure 4.10).

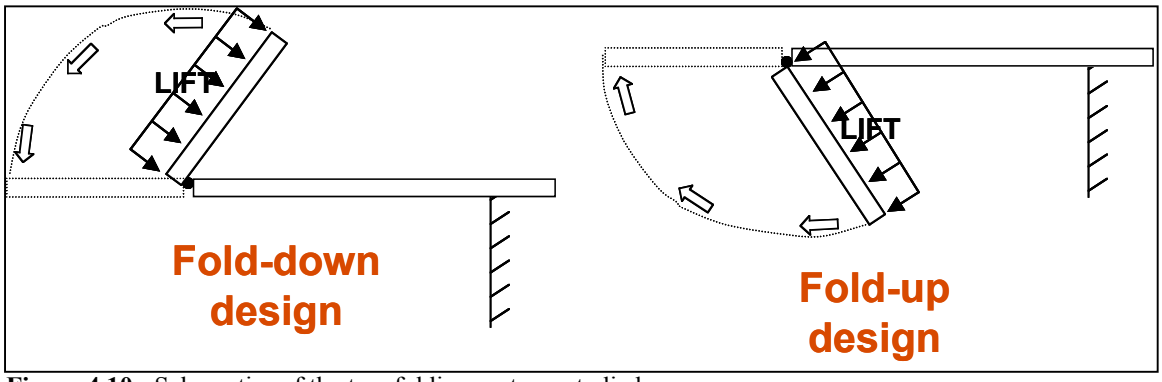

Figure 4.10: Schematics of the two folding systems studied

By way of inspection, the fold-down design was immediately ruled out because of the difficulty that arises from folding the wing section against its own lift force. The forcing system required by this design, such as hydraulics or pulleys, would add a high level of sophistication and weight to the concept. In addition, the point forces and/or bending moments that the folding wing would be required to endure are much too great for the intended simple wing structure.

The fold-up design was determined to be a feasible option at first because the lifting force on the folding section would assist in the folding. Therefore, a small analysis was performed on the dynamics of the folding section. In the analysis, the bending moment caused by the rotation of the section was determined using Equation 4.9:

$$\sum M_{hinge} = \bar{I}\alpha + m\bar{a}d \qquad \textbf{EQN 4.9}$$

where I is the mass moment of inertia, _ is the angular acceleration, m is the mass of the rotating section, a is its linear acceleration, and d is the distance from the axis of rotation to the center of mass. It was determined that for stability purposes after launch, the full wing section would need to be in place in 1.5 seconds. Therefore, the wing section would need to rotate about 120º in 1.5 seconds, giving an angular acceleration of 80º/s^2. Using this value, and assuming the section to be constructed of 0.05" thick Aluminum 2014 T6 alloy, the moment experienced by the hinge at the time of locking would be 37.7 ft-lb.

Comparison with the structural analysis of the wing indicated that at the half span position the conventional winged concept is expected to have a bending moment due to normal lift of 30 ft-lbs. Thus,

the additional 37.7 ft-lb moment imparted by the rotating wing section would more than double the bending moment carried by the wing. In the design of aircraft wings, the bending moment is the driving force in the structural sizing of the wing. Consequently, this doubling of the bending moment would require twice as much wing strength as a non-folding design. This increase in wing strength would come with a large penalty in weight.

The previous moment analysis does not take into consideration the large impulse received by the inboard section of the wing during locking. To reduce the large impulse transmitted through the wing at locking, a damper system would need to be implemented. Introduction of a damper system into the wing would necessarily add cost, weight, and complexity to the design.

In conclusion, the study of the folding wing concept brought forth certain drawbacks in the design that were not discovered in the initial evaluation of the concept. Specifically, the large moments created in the wings during the locking procedure requires a much larger and stronger wing structure than a non-folding wing. This increase is wing strength will result in increased weight and cost over a non-folding wing design.

A brief study of the merits of the scissor wing design was performed for comparison with the results from the folding wing study. Figure 4.11 is a schematic of how the scissor wing concept would work. As shown in the figure, the wing is mounted to the fuselage by way of a metal rod running from the top to the bottom of the fuselage. The top end of the rod would be attached to a load distributing plate or rod inside the wing.

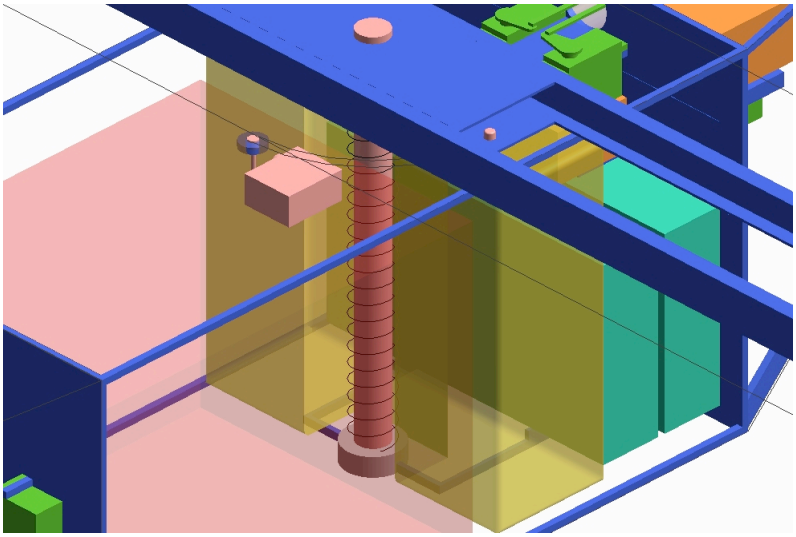

Figure 4.11: Schematic of scissor wing concept.

Observation shows that the scissor wing concept does not subject the aircraft wing to additional loads or moments beyond those encountered in normal flight. Through proper design of the interface between the pivot rod and wing root, the moments and loads the wing is subjected to will be comparable to those encountered by a wing simply connected to the fuselage. Therefore no additional strengthening of the wing would be necessary. Consequently the scissor wing concept does not suffer from the weight or cost penalties of the folding wing design and is therefore the preferred method of variable wing geometry.

4.11 Final Selection

To decide on the final design, the team developed four factors of merit to judge the design concepts. The first factor of merit is weight, which tells us the amount of materials needed for construction to give us an idea on materials costs. The second factor of merit is manufacturing costs, or the cost effectiveness of the design concept in mass production. The third factor of merit is the drag coefficient C_d at loiter, which plays a major role in fuel consumption and engine selection. The fourth and final factor of merit is power required, which is the size of the engine needed for loiter flight.

Each of these factors was assigned a weighting value and a decision matrix was created with the actual values of each factor of merit entered into the matrix. The decision matrix is shown in Table 4.5. The averages were taken for each set of data and divided into each data

point to normalize the data. The normalized scores were multiplied by the weighting values, and the resulting values for each factor of merit of the designs were added to produce a final ranking.

The normalized decision matrix is shown in table 4.6. It should be noted that a low score in this system is better, since the optimum values for each factor of merit are less than one. Table 4.6 shows that the scissor wing concept received the lowest score in the decision matrix. Consequently, the scissor wing concept was selected for detailed design.

Table 4.5: Decision matrix utilizing raw data.

FOMs	Delta	Folding	Scissor	Average
Weight (lbs)	193	187	187	189
Manufacturing Costs	6	7	4	5.7
Cd at Loiter	0.0861	0.0498	0.0498	0.0619
Power Required (hp)	7.29	4.21	4.21	5.24

Table 4.6: Normalized UAV concept decision matrix

Normalized Decision Matrix			
FOMs	Delta	Folding	Scissor
(4) Weight (lbs)	1.021	0.989	0.989
(5) Manufacturing Costs	1.059	1.235	0.706
(2) Cd at Loiter	1.392	0.804	0.804
(3) Power Required (hp)	1.392	0.804	0.804
Total	16.338	14.155	11.508

Chapter 5 Final Configuration

In order to give a better idea of what the Team Lemming CUAV looks like, this section provides a number of views of the aircraft. These will clarify servo mounting locations, tail and wing mounting details, as well as the 3Dimensional location of all the systems. Two more drawings of the tail mounting and the aileron mounting are available in chapter 12.

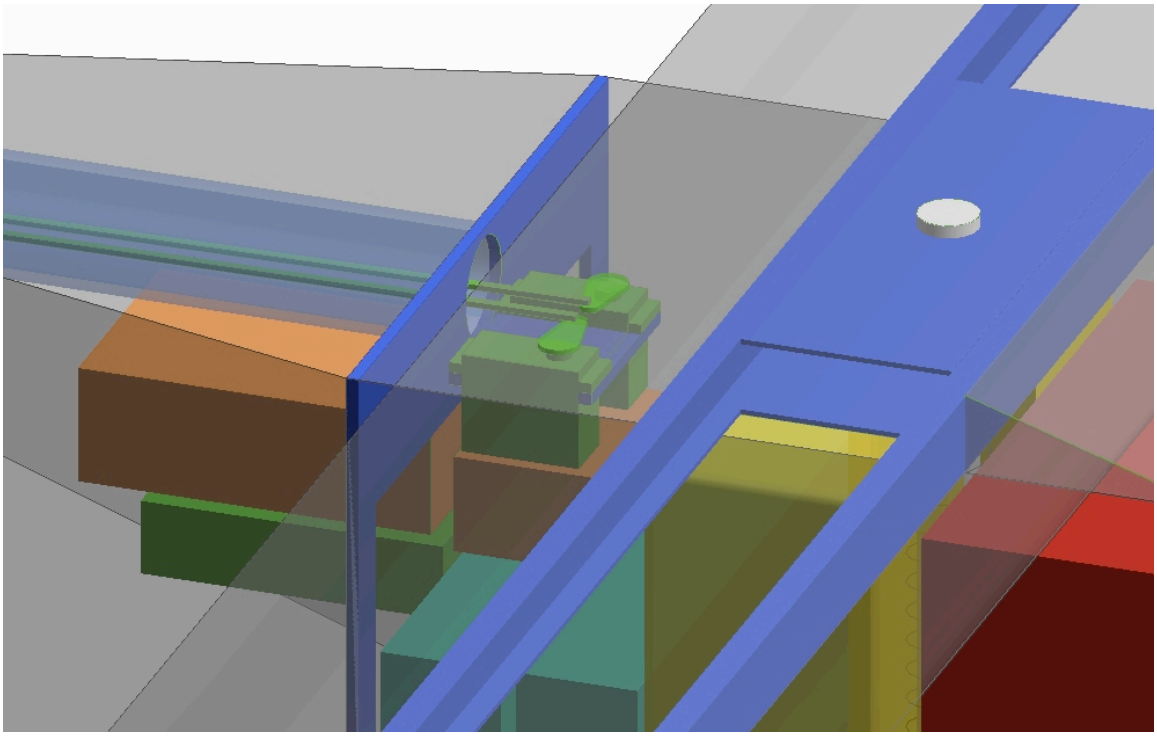

Figure 5.2: Tail Servo Details.

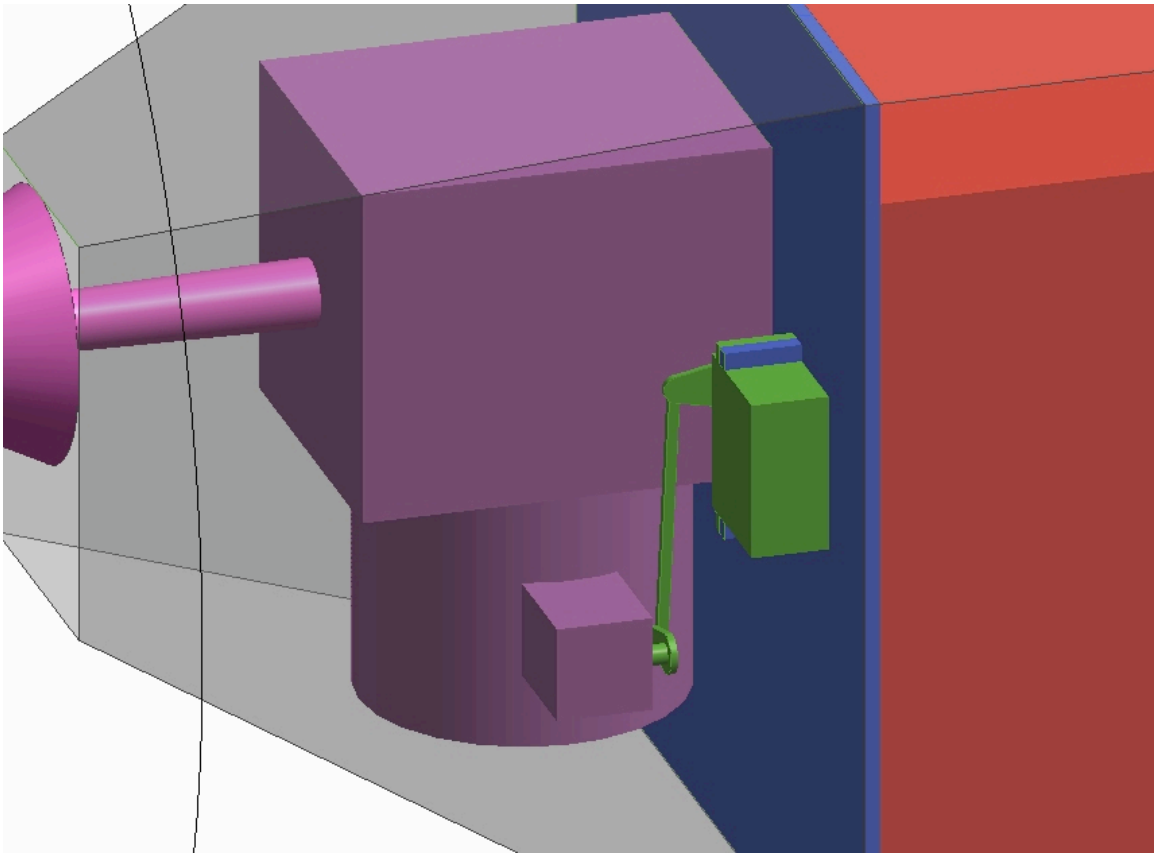

Figure 5.3: Throttle Servo mounting detail.

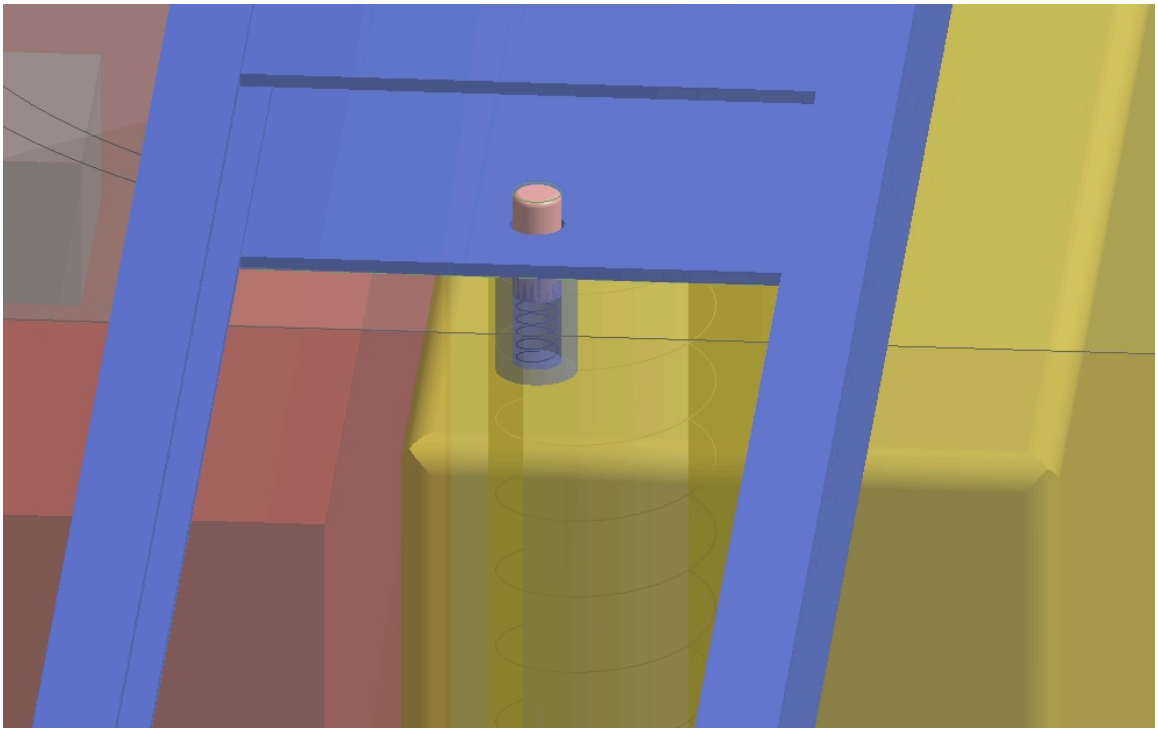

Figure 5.4: Wing swivel catch pin detail.

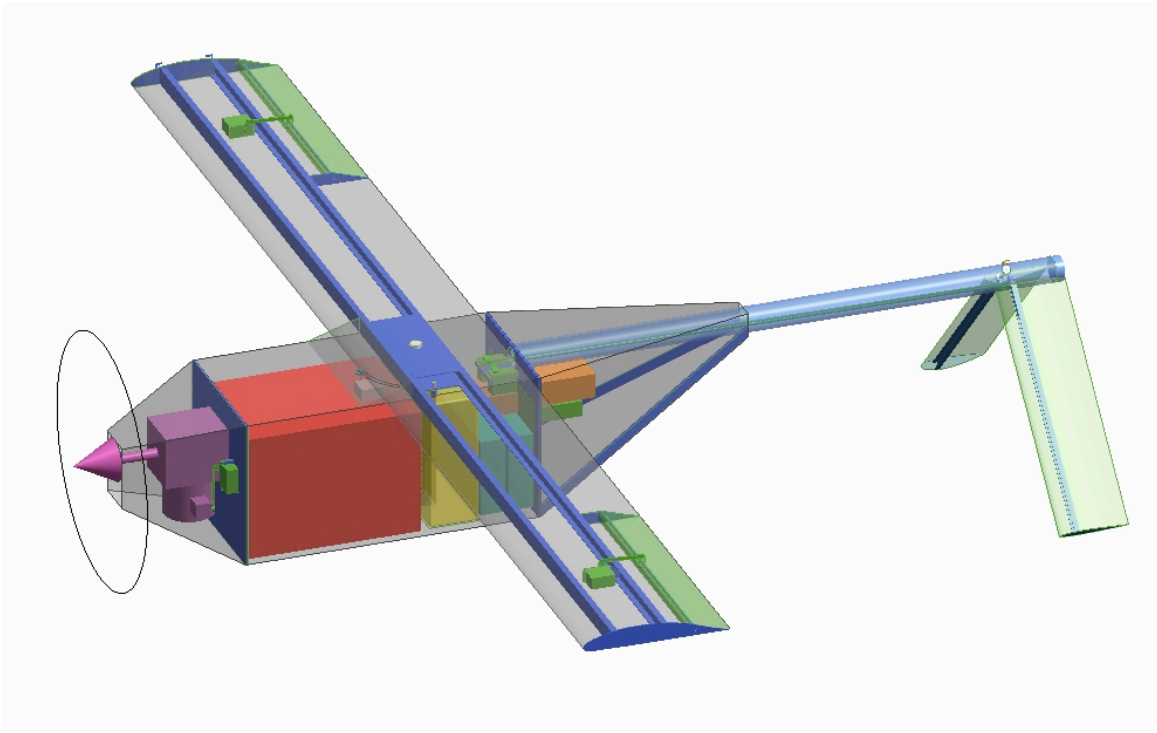

Figure 5.5: Three dimensional layout of aircraft.

Chapter 6 UAV Performance

6.1 Performance Overview

Creation of performance parameters for the CUAV was largely at the discretion of the group because the aerial performance of the CUAV was unspecified by the RFP. The only requirement the CUAV must meet to satisfy the RFP is the endurance requirement of 5 hours. Also, because the CUAV is an un-manned vehicle, it is exempt from MIL and FAR flight performance specifications. Furthermore, due to the expendable nature of the CUAV mission and the team's choice of aerial launch methods, field performance is a moot point. Consequently, the group was responsible for developing the minimal up-and-away performance of the craft, which consisted of rate of climb and level-flight performance characteristics.

The minimum level flight requirements set by the group were that the CUAV must be capable of maintaining level flight at all altitudes between sea-level and the design ceiling of 10,000 ft. Furthermore, the CUAV must be able to loiter at all altitudes up to and including 10,000 ft for a minimum period of 5 hours. The team also required minimal rates of climb at sea-level and 10,000 ft of altitude. These requirements were a minimum ROC of 200 ft/min at S.L. and a 100 ft/min ROC at 10,000 ft.

The original performance requirements were analyzed to determine the minimum engine size required to meet the requirements. A detailed description of this analysis is given in reference 6.1. The results of the engine sizing study indicated that a 6.2 Hp engine would be required to power the UAV, with the governing factor being the 100 fpm ROC at 10,000 ft. However, in the detailed design phase, the group chose to use an engine with a nominal horsepower of 14.8. Consequently, all of the original requirements are more than exceeded by the CUAV.

6.2 Rate of Climb

Maximum rate of climb for a propeller powered craft occurs at the minimum power velocity. The minimum power velocity, Vmp was calculated by equation 6.1 from Raymer.[6.2] For this equation, the constants K ($1/\pi ARe$) and Cdo were calculated from the drag polar given in chapter 9.

$$V_{mp} = \sqrt{\left(\frac{2W}{\rho S}\sqrt{\frac{k}{3C_{Do}}}\right)} \qquad \textbf{Eqn 6.1}$$

Once the minimum power velocity for a given altitude was known, the maximum rate of climb was calculated by equation 6.2, which also came from Raymer[6.2]. In Eqn 6.2, bhp is the available horsepower of the engine at altitude as determined by equation 8.1 from the propulsion chapter, and the propeller efficiency (_p) is taken as 0.79. The resulting rates of climb are given in table 6.1. As shown in the table, the CUAV easily exceeds the original design team climb requirements.

$$ROC = \frac{550 bhp \eta_p}{W} - \frac{DV}{W} \qquad \textbf{Eqn 6.2}$$

Altitude	Max Rate of Climb
Sea Level	2211 fpm
5,000 ft	1684 fpm
10,000 ft	1277 fpm

Table 6.1: CUAV maximum rate of climb

6.3 Flight Envelope

The level flight envelope for the CUAV was calculated. The flight envelope consists of all speeds over which the CUAV can maintain level flight over a range of altitudes. The boundaries of the flight envelope are the stall boundary and the maximum power boundary. The stall boundary is the minimum speed at which the airfoil can create enough lift to support the UAV. The power boundary is the maximum speed at which the engine can offset the drag of the UAV at a given altitude.

The stall boundary was calculated using equation 6.3. For the stall boundary equation a Cl_{max} of 1.57 was used, as calculated in the aerodynamics chapter.

$$V_{\min} = \sqrt{W / Cl_{\max} \, 0.5 \rho S} \qquad \textbf{Eqn 6.3}$$

The power boundary was calculated by setting the power available from the engine equal to the power required to offset the drag of the CUAV. Power available equals the maximum engine power at each altitude as listed in chapter 8 multiplied by the propeller efficiency of 0.79. The power required was calculated using equation 6.4. In equation 6.4, Cdo and k were determined from chapter 9. A Matlab

function was written to iterate different velocities in equation 6.4 until the power required at a given altitude equaled the power available. The level flight envelope, defined by the stall and power boundaries, is shown in figure 6.1. Figure 6.1 also shows that the ceiling of the CUAV is 25,000 ft.

$$P_r = \left[C_{do} + k \left(W / 0.5 \rho V^2 S \right)^2 \right] 0.5 \rho V^2 S \qquad \textbf{Eqn 6.4}$$

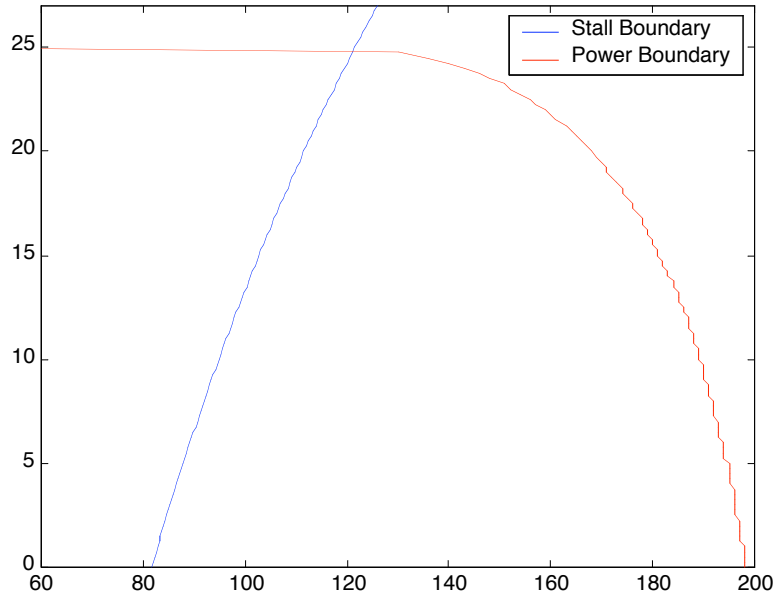

Figure 6.1: Flight envelope for CUAV

6.4 Range and Endurance

Range and endurance estimates for the CUAV were complicated by the fact that an accurate specific fuel consumption constant is not known. The only data found for the fuel consumption of the engine is a rate of 0.53 gal per hour, which was learned through personal communications[6.3]. It is unknown at what conditions this rate applies. For calculation purposes, the group assumed that the stated rate would occur at 30% of engine power. The group further assumed that fuel consumption would be proportional to the amount of full power used at a given flight condition. Consequently, the normal equations for estimating range and endurance could not be applied to the UAV. The group was forced to use crude approximations to estimate range and endurance.

The CUAV is designed for a reconnaissance mission. Consequently, the CUAV is flown to optimize loiter time on target. To maximize endurance, a propeller powered airplane should fly at the Cl and velocity where the aircraft uses a minimum amount of power. The minimum power velocity is calculated by equation 6.1, which was given earlier in this chapter. Once the velocity for minimum power was known, equation 6.5 was used to solve for the Cl for min power.

$$Cl_{mp} = W / 0.5 \rho V_{mp}^2 S \qquad \textbf{Eqn 6.5}$$

The Clmp was used to find the drag coefficient and corresponding drag at a given altitude for minimum power. Drag was multiplied by velocity to determine the power required. The power required was divided by the engine power available to determine the fraction of engine power used. Fuel consumption was assumed to be proportional to the engine power fraction. Endurance was taken to be the engine burn time for the estimated fuel consumption, while the range while flying at minimum power was estimated as the burn time multiplied by the minimum power velocity. The range and endurance results are summarized in table 6.2

Altitude	Min Power Vel	Drag	Power Req'd	Est. Fuel Cons.	Endurance	Range
Sea Level	111 fps	9.05 lbs	1.83 Hp	0.28 gal/hr	11.7 hr	880 mile
5,000 ft	120 fps	9.09 lbs	1.98 Hp	0.37 gal/hr	8.6 hr	705 mile
10,000 ft	129 fps	9.029 lbs	2.12 Hp	0.48 gal/hr	6.7 hr	590 mile

Table 6.2: Range and endurance results for the CUAV operating at loiter conditions.

Chapter 7 Missions Analysis

The CUAV is intended to fulfill a very simple mission profile. The UAV is designed to launch from a Navy aircraft or ship at an altitude either equal to, below, or above the mission altitude. If deployed above the mission altitude, the CUAV will simply descend in the idle throttle setting or float down on the deployment parachute in the parachute deployment mode. If launched from below the mission altitude, the CUAV will climb to the desired altitude and begin the reconnaissance flight. Depending on the reconnaissance instrumentation onboard, the mission altitude is assumed to be between 5,000 and 10,000 ft. Below 5,000 ft the probability of having the CUAV shot down by enemy fire is very high. Above 10,000 ft, the low cost reconnaissance equipment used on the CUAV becomes ineffective.

Once the specified mission altitude is reached, the CUAV will either begin the reconnaissance part of the mission, or will begin a cruise segment to the target area. Although the performance section of this report indicates dash speeds for the CUAV well in excess of the design loiter velocities, the cruise segment of the mission will be performed at the minimum power setting to reduce fuel consumption. Consequently, once the climb or descend segment of the flight is completed the CUAV will fly at the minimum power setting for a given altitude for the duration of the flight, which are given in table 6.2. However, this desire to conserve fuel would of course be violated if speed to reach a target site was more important than time over the target.

Figure 7.1 shows a graphical representation of the design mission profiles for the CUAV. As shown in the figure, at the design altitudes below 10,000 ft the CUAV has a total minimum endurance of 6 hours. This is well in excess of the 5 hours on station required by the RFP.

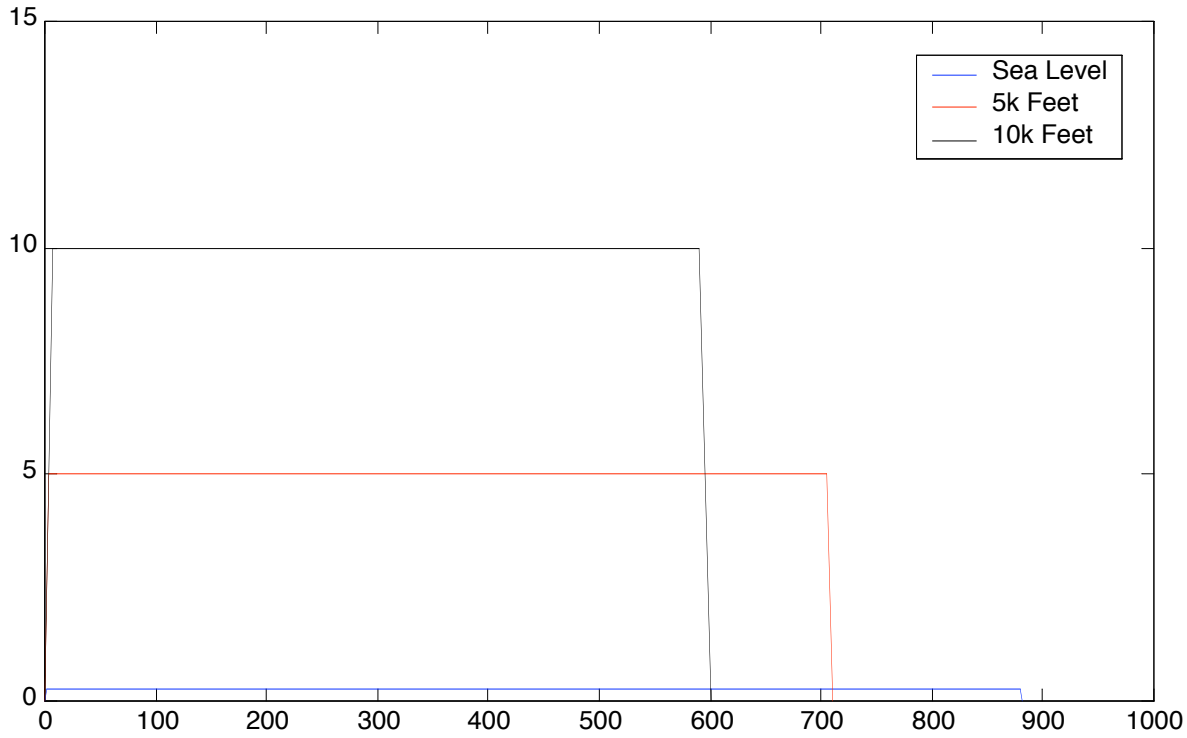

Figure 7.1: Mission profile for Cheap UAV.

Chapter 8 Propulsion

8.1 Propulsion Selection

Using the required horsepower calculation for a 200 fpm climb at 5000 feet of 5.85 hp, we now have enough information to select an engine for our UAV. Three variables were considered when selecting an engine: horsepower, size, and cost. The engines considered were R/C piston engines and standard horizontal shaft piston engines.

The first engines looked at were standard horizontal shaft engines, specifically the Tecumseh Power Sport and the Honda GX270 QAE2. These engines, shown in figures 8.1 and 8.2, are four stroke engines rated at 10 hp and 9 hp respectively, with an electric starter included with the Honda. Both engines had low costs of $495.99 and $742.50 respectively but with weights of 55 and 62 lbs, other alternative would have to be found.

www.tecumsehpower.com

Figure 8.1: Tecumseh Power Sport

www.planopower.com

Figure 8.2: Honda GX270 QAE2

The next engine looked at was the Saito FA-450R3-D, shown in figure 8.3. This small 4 cycle engine, weighing only 6.5 lbs, provides 7 hp at 8000 rpm with 1/10 the normal vibration of comparable engines, all at the cost of $1069.95. The reduction in vibration means less noise and a less chance that a part of the aircraft would break due to fatigue, both important to our mission. An electric starter would have to be purchased and fitted to the engine since one is not included.

horizon.hobbyshopnow.com

Figure 8.3: Saito FA-450R3-D

The next engine looked at is the Fuji BT-86 Twin, shown in figure 8.4. Similar to the Saito engine, the Fuji engine weighs 6.2 lbs, has 7.5 hp, and costs $1200.00. An electric starter will also have to be purchased for this engine, since one is not included. However this engine is a two-cycle, meaning it runs on a fuel-oil mix. The additional power and less weight at only a slightly increased cost make this engine slightly more favorable.

www.fujiengines.com

Figure 8.4: Fuji BT-86 Twin

www.radne.se

Figure 8.5: Raket 120 Aero E

Although the two previous engines are both extremely lightweight and meet the horsepower requirement, they barely meet the horsepower requirement. This means maneuverability will be at a minimum. The next engine, the Raket 120 Aero ES, shown in figure 8.5, has 14.8 hp, weighs 15 lbs, and costs only $1100.00. The added power improves the performance of the UAV significantly with only an 8 lb increase in weight. This two-cycled engine also includes an electric starter. Based on this analysis, the Raket 120 Aero ES built by Radne Motor AB is the engine selected for our design. Specifications for this engine are shown in Table 8.1 and altitude adjusted power is shown in Table 8.2. Altitude Adjusted power was calculated using equation 8.1 from Raymer[8.1]:

$$\text{power} = \text{power}_{SL} \_ (\_/\__0 - (1 - \_/\__0)/7.55) \qquad \textbf{EQN 8.1}$$

Table 8.1: Engine specifications for Raket 120 Aero ES

Type of Engine	One Cylinder Two-Stroke Engine, Piston Control of Inlet
Cylinder Volume	7.25 in^3
Stroke	1.65 in
Bore	2.36 in
Cooling	Fan Cooled
Ignition	Transistor
Power	14.8 hp at 9000 rpm
Max rpm	13000 rpm
Weight	15 lb
Carburetor	Walbro
Clutch	Centrifugal
Fuel Consumption	0.53 gal/h

www.radne.se

Table 8.2: Altitude adjusted power

Height (ft)	Adjusted Power (hp)
Sea Level	14.80
1000	13.62
2000	13.17
3000	12.73
4000	12.30
5000	11.87
6000	11.46
7000	11.06
8000	10.67
9000	10.29
10000	9.91

8.2 Propeller Selection

The propeller selection method used is outlined in Raymer, pages 395-398.[8.1] The advance ratio was found using the equation:

$$J = V/nD \qquad \textbf{EQN 8.2}$$

Where n is rotation speed and D is the propeller diameter. The power coefficient was calculated using the equation:

$$c_P = 550\ bhp/\_n^3D^5 \qquad \textbf{EQN 8.3}$$

where bhp is the brake horsepower. Using figure 13.12 in Raymer[8.1], the propeller efficiency $\__p$ can be estimated. It should be noted that figure 13.12 assumes an activity factor of 100 and a blade design C_L of 0.5, which typical values and both true for our design. Also, the figure is for three-bladed propellers, where ours will be a two-bladed propeller to allow for a larger diameter. To make the correction, the

estimated η_p is multiplied by 3%. Once the propeller efficiency is found, the thrust and thrust coefficient can both be found. The equation used to calculate the trust created by the propeller is:

$$T = P\eta_p/V \qquad \textbf{EQN 8.4}$$

Once the thrust is found, the thrust coefficient can be found using:

$$c_T = T/\rho n^2 D^4 \qquad \textbf{EQN 8.5}$$

The speed-power coefficient can also be found and since it does not require propeller diameter, is useful in comparing propellers of different sizes. It is calculated using the equation:

$$c_S = V(\rho/Pn^2)^{1/5} \qquad \textbf{EQN 8.6}$$

Table 8.3 shows the propeller sizing calculations with various rotational speeds and propeller diameters.

Table 8.3: Propeller sizing chart

Diameter (ft)	Rotation Speed (rev/s)	Advance Ratio	Power Coef.	Propeller Efficiency	Speed-Power Coef.	Thrust	Thrust Coef.
2.0	66.67	1.0125	0.3610	0.53	1.2048	31.96	0.2194
2.0	75.00	0.9000	0.2536	0.68	1.1493	41.00	0.2224
2.0	83.33	0.8100	0.1848	0.75	1.1019	45.22	0.1987
2.1	58.33	1.1020	0.4222	0.48	1.2709	28.94	0.2135
2.1	66.67	0.9643	0.2829	0.65	1.2048	39.19	0.2214
2.1	75.00	0.8571	0.1987	0.78	1.1493	47.03	0.2099
2.1	83.33	0.7714	0.1448	0.78	1.1019	47.03	0.1700
2.2	58.33	1.0519	0.3346	0.63	1.2709	37.99	0.2327
2.2	66.67	0.9205	0.2242	0.73	1.2048	44.02	0.2064
2.2	75.00	0.8182	0.1574	0.8	1.1493	48.24	0.1787
2.3	58.33	1.0062	0.2679	0.75	1.2709	45.22	0.2319
2.3	66.67	0.8804	0.1795	0.83	1.2048	50.05	0.1965
2.3	75.00	0.7826	0.1261	0.83	1.1493	50.05	0.1552
2.4	50.00	1.1250	0.3439	0.63	1.3517	37.99	0.2236
2.4	58.33	0.9643	0.2166	0.78	1.2709	47.03	0.2034
2.4	66.67	0.8438	0.1451	0.83	1.2048	50.05	0.1657

It was decided that propeller efficiency should be at least 75% and that the propeller should be as small of a diameter as possible to reduce costs and help in storage. Although the 2 foot diameter propeller with a rotation speed at 83.33 rev/sec meets these requirements, by increasing the diameter to 2.1 feet and decreasing the rotation speed to 75.00 rev/sec, we get a more optimum propeller. If we increase the diameter to 2.2 feet and keep the rotation speed the same, we get a more efficient propeller, however the

power and thrust coefficients both decrease. Thus this analysis concludes that a propeller with a diameter of 2.1 feet and a rotation speed of 75.00 rev/sec is the optimum propeller for our design.

www2.towerhobbies.com/

Figure 8.6: Zinger 26_10 wood propeller.

Materials propellers are constructed from include; wood, carbon fiber, glass fiber, plastic, and metal. Carbon fiber, glass fiber, and metal are fairly expensive and plastic is not strong enough for our requirements. Wood propellers are strong enough and cheap and will be the material of choice. However, so many propellers on the market fit our requirements such that it is impossible to look and compare all of them. Looking at some of the better known manufactures (such as APC, Master Airscrew, Top Flight, and Zinger), the Zinger 26_10 wood propeller shown in figure 8.6 has the lowest cost for the quality we need.

Chapter 9 Aerodynamics

Throughout the course of the development of the CUAV, the Aerodynamics team was assigned several tasks. The first of these was to perform a preliminary analysis of the three selected UAV concepts. Once the final concept had been chosen, the airfoil selection process was initiated in a quest for a simple, yet sufficiently high performance design. Once the airfoil was selected, the wing design was optimized. With these tasks completed, the team set out to develop a detailed model of the aircraft's drag. The work of the Aerodynamics team was used by other facets of the team in the determination of the motor requirements, the endurance and ROC of the aircraft, and the structural requirements of the wing.

9.1 Preliminary Analysis

The drag of the three preferred concepts was important to the selection of the final concept. This analysis was simplified by the fact that the scissor wing and folding wing concepts had the same fuselage and wing dimensions; therefore the analysis was broken into Conventional and Delta concepts. The program Friction.f[9.1] was used to provide the aerodynamic comparison of the preferred concepts. Three different flight regimes were investigated: the maximum speed at loiter altitude (h = 5kft, V = 140kts);

the loiter speed at loiter altitude (h = 5kft, V = 80kts); and the loiter speed at maximum ceiling (h = 10kft, V = 80kts). In other words, Mach number and altitude were used to define the three flight states. The wetted areas of the concepts were found using the concept drawings, and the wing wetted area was estimated at twice the wing area. The wetted area of the delta wing's payload area (box cross-section portion) of the fuselage was calculated on three sides, since the third side is covered entirely by the wing. The delta wing was found to have 50.687 ft^2 of wetted area, while the conventional and scissor wing concepts had 52.46 ft^2 of wetted area. The fuselages were assumed to be turbulent due to the foreward tractor propeller. The wings' transition was forced at 0.3% of the chord, which is the location of maximum thickness on 4 digit series airfoils. The forced transition of the wings was done to give a realistic estimate of the amount of laminar flow that the wings might exibit. Table 9.1 gives the results from the friction program, as well as a calculation of the total drag of the concepts at the 3 flight conditions. This table also holds validation data, which was taken from the 2001-2002 VT DBF competition airplane. The top speed of this aircraft was found to be 47 mph, based on calculations of the time the aircraft took to fly a lap at competition and the estimated lap length. The team had access to propulsion data of the Astro Cobalt 60 motor with a 22 x 12 propeller taken by Dzelal Mujezinovic in the Virginia Tech Open Jet Wind Tunnel, showing a maximum thrust of 1.5 lbs at 47 mph. As can be seen from Table 9.1 this shows that the friction program overestimated the drag by 0.3lbs, a 20% overestimation, which is acceptable during the preliminary estimation of the concepts.

Table 9.1: Drag Estimation and Validation

	Delta	Conventional	DBF 1
Cdo Case1	0.0158	0.0160	0.0151
Cdo Case2	0.0177	0.0181	
Cdo Case3	0.0182	0.0186	
C_L Case1	0.2649	0.2707	0.6439
C_L Case2	0.8115	0.8036	
C_L Case3	0.9441	0.9349	
Cdi Case1	0.0058	0.0029	0.0156
Cdi Case2	0.0547	0.0257	
Cdi Case3	0.0741	0.0348	
Cd Case1	0.0216	0.0189	0.0307
Cd Case2	0.0725	0.0437	
Cd Case3	0.0923	0.0533	
D Case1	15.7250	13.7831	1.8503
D Case2	17.2334	10.4034	
D Case3	18.8686	10.9033	
case1: V = 140kts, h = 5kft			
case2: V = 80kts, h = 5kft			
case3: V = 80kts, h = 10kft			

9.2 Airfoil Selection

With the final concept selected, the Aerodynamics team decided that determining the airfoil of the CUAV was the first priority during detailed design. Selecting the airfoil would allow the wing structures to be designed, as well as determine if the wing could allow optimization. The airfoil for this design would need to be inexpensive to construct, and have a high L/D, to meet the RFP. Because minimization of cost was paramount, a flat-bottomed airfoil would be advantageous to reduce production costs. Currently the only available flat-bottomed airfoil available is the Clark Y, designed by Col. Virginius E. Clark in 1922[9.2]. Since 1922 there has been a significant amount of research in the area of Natural Laminar Flow Airfoils (NLFs), which would help raise the maximum L/D of a flat-bottomed airfoil. In order to reap these benefits the team decided there was the need of a new airfoil for the design. This new airfoil would need to have better aerodynamics than the Clark Y airfoil, while maintaining a flat-bottomed lower surface over at least 25% of the chord. The improved aerodynamics included either lower drag at cruise or a higher L/D at cruise, and a C_{lmax} greater than or equal to that of the Clark Y.

The XFOIL 6.94 program was used to compare the drag and lift polars of the new airfoil to the Clark Y at the design criterion. This criterion called for a minimum cruise C_l of 0.8 at a speed of 135 fps, and at an altitude of 5,000 feet. This C_l was found using the L/D max of a NACA 4412 airfoil[9.3], which was the airfoil that provided the basis for wing sizing during the Preliminary Design phase of the wing. This resulted in a wing with a span of 10 ft, and a chord of 14 inches. The design points were used to calculate the wing's Reynolds Number, which is important to accurately predict the airfoil's performance. Using the equation:

$$\mathrm{Re} = \frac{\rho V c}{\mu} \qquad \textbf{EQN 9.1}^{9.4}$$

The Reynolds number was found to be 8.8 x 10^5. Thus, during cruise, the wing will be at the upper limit of the Low Reynold's Number range. It is also advantageous to factor in the Mach Number, M, that the UAV is cruising at. Hence the following equation:

$$M = \frac{V}{a} \qquad \textbf{EQN 9.2}^{9.4}$$

The speed of sound, a, at 5k ft was found using an online Atmospheric Table[9.5] to be 1097.09 fps. This resulted in an M of 0.1231.

A limited amount of time was available to the author to create the new airfoils. This meant that an exhaustive search for Natural Laminar Flow (NLF) airfoils was not feasible. Instead, the author was restricted to searching the UIUC Airfoil Coordinates Database[9.6]. Using this database would eased author's work load because the coordinates were already saved in electronic file types, requiring very little manipulation to load them into XFOIL. The airfoils were selected by finding all the NASA/Langley airfoils that were either NLF, or General Aviation. The General Aviation airfoils were considered because of their higher thicknesses, and because their profile allowed for a grafted flat section easier. These airfoils were then whittled down to three airfoils that were the most practical to this study, the NASA\Langley: NLF(1) 0115, NLF 414f; and the LS(1)-0417. These final airfoils were chosen to exibit a range of thicknesses and shapes. Their contours can be seen in Figure 11.1, along with that of the Clark Y.

With a list of candidate airfoils the author could begin adapting the airfoil profiles. The first method used was the INTE function in XFOIL, where two airfoils were selected, the Clark Y and an NLF airfoil, to be morphed together by the XFOIL program. The team could choose the amount of each airfoil to be used in the combination process. A Clark Y bias was used so that a flat bottom would be preserved. The next method used was to graft in a flat section on the bottom of an NLF airfoil, ranging in length from 20% to 65% of the airfoil chord. The grafting was done in Matlab, and then the transition from the old curve to the flat section was smoothed using XFOIL's function pressure distribution design menu MDES. After this an attempt was made to use a Low Reynolds number (Re) airfoil, with a grafted flat section. The final method used to create a better flat-bottomed airfoil was to combine the Clark Y flat-bottom coordinates with new NLF upper surface coordinates. For each method several examples were tried so that a trend could be noticed, before the next method was tried.

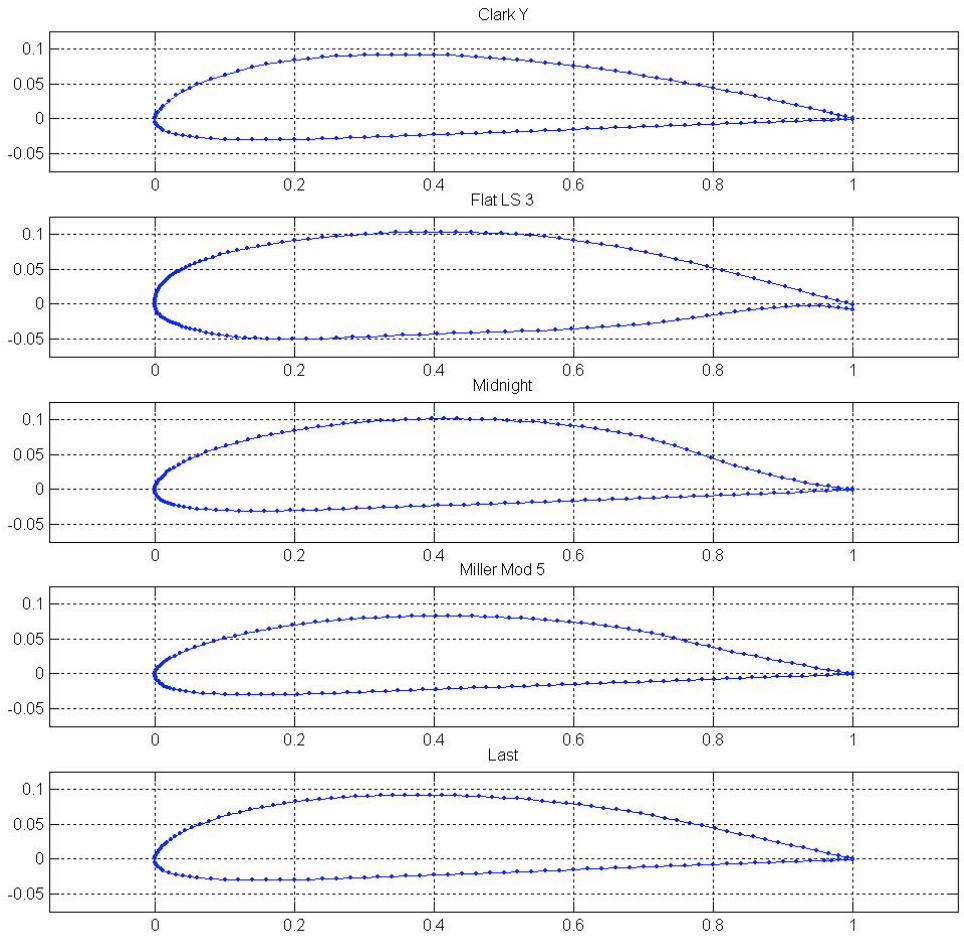

Figure 9.1: Contours of airfoils investigated for CUAV project.

During this research a total of 28 airfoils were produced, many of them being simple stepping stones, of which 5 were presented to the team for evaluation. These were the Clark Y, the Flat LS 3, the Miller Mod 5, the Midnight, and the Last. Figure 9.2 is a polar plot comparing these airfoils, Figure 9.1 is a plot of the contours of these airfoils, and Table 9.2 has the basic performance comparison of the 5 airfoils. The Clark Y has proven it is a tough airfoil to beat in

ease of building, not to mention its wide range of low drag. The Last airfoil is a good successor to the Clark Y, showing improvements in both cruise and climb performance. The Midnight

Table 9.2: Airfoil Characteristics

	L/D max	Cl of L/Dmax	Cd of L/Dmax	Clmax	t/c
Clark Y	111.54	0.75	0.00672	1.5	11.71%
Flat Ls 3	110.44	0.8	0.00724	1.77	14.65%
Midnight	154.88	0.875	0.00565	1.6	12.67%
Miller Mod 5	137.02	0.7	0.00511	1.4	10.70%
Last	125	0.75	0.006	1.55	11.87%

airfoil exibits a very high L/D, which would be beneficial to the endurance requirements on the CUAV. The Miller Mod 5 has a nice dip in drag around 0.7 C_l, and might be useful in designs where C_{lmax} is not important, or in an aircraft with a cruise Re in the range of 500,000 or 600,00. Finally, the Flat Ls 3 airfoil is recommended in projects where minimal structural weight and increased C_{lmax} is important.

After discussing the pros and cons of the airfoils with the rest of the team, the Midnight airfoil was finally selected. This airfoil was selected for several reasons. Most importantly, the Midnight airfoil has a superior L/D, and it is one of only two airfoils that has its L/D_{max} at a C_l equal to or greater than 0.8. In addition, the upper surface is shaped so that at the 60% chord the airfoil is thick enough that the two wing spars can be identical.

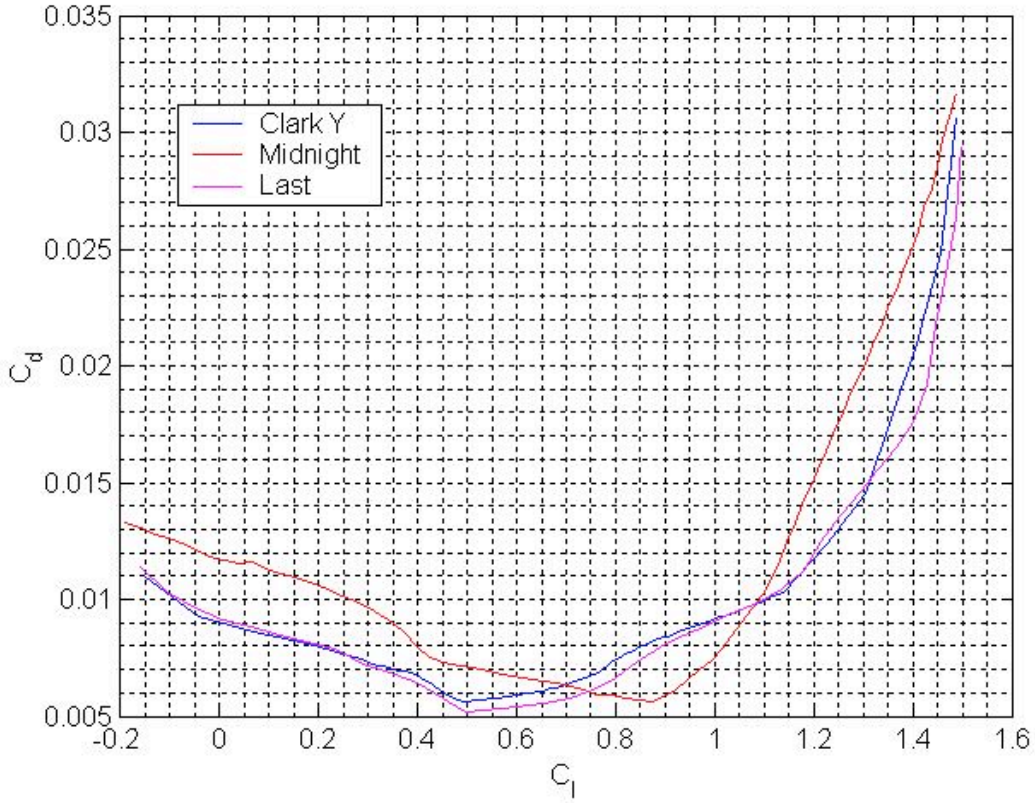

Figure 9.2: Drag polars for Clark Y, Midnight, and Last airfoil

9.3 Drag Buildup

With the airfoil selected the size of the wing needed to be optimized, which required an analysis of the drag trade-off of using a smaller wing. Because the Midnight airfoil had such a high L/D, the team found that the wing area could be dropped 0.5 ft^2 and still provide the required lift at maximum flight weight of 140 lbs. Part of this reduction in wing area also came from further analysis of the structure and system components that made up the CUAV, resulting in a total vehicle weight of around 30 lb less than originally estimated. Despite this weight drop, and the improved performance of the airfoil, the Aerodynamics team decided to keep the wing dimensions the same. Part of the reason for this was by not reducing the wing area, a longer wing span would reduce the induced drag of the wing. A simple drag build up was done to compare a CUAV with a 1ft reduction in span with a CUAV with the 10 ft span. The team found that the maximum L/D of dropped from 13.36 for the 10 ft span to 12.00 for the 9 ft span. This analysis also didn't include trim drag from the tail, which would probably make the disparity in the

two L/Ds worse. For these reasons the team kept the wing the dimensions determined in the preliminary design.

The Aerodynamics Team used the simple drag build up to produce an Excel file including trim drag. This provided a better drag model for the performance team. This file used the Midnight and NACA 0009 airfoil polars calculated in XFOIL for their respective flight Re. Also used was a recalculation of the fuselage Cdo in Friction[#] of 0.0156, which included both form and friction drag

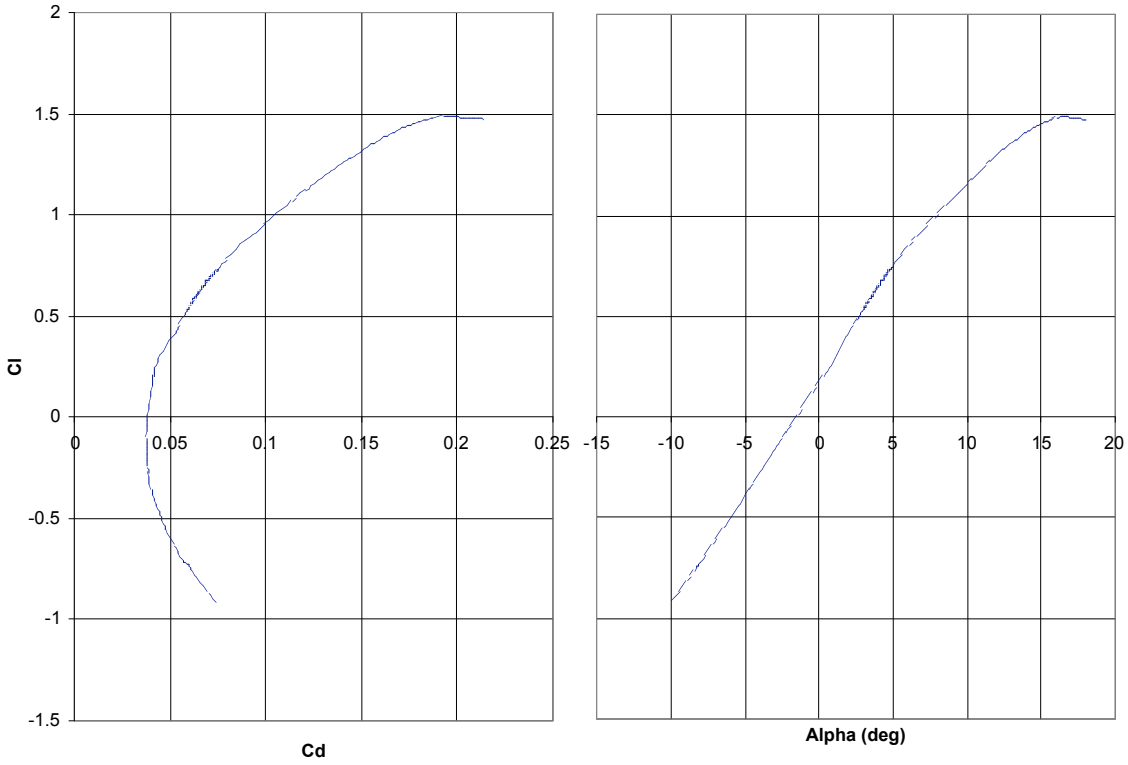

Figure 9.3: Lift and Drag Polar of Trimmed CUAV

components. The induced drag of the wing was calculated with the Midnight airfoil polar at each angle of attack. The induced drag was added to the Cdo value of the wing airfoil at that angle of attack. Next the lift coefficient required at the tail, Clt, was calculated based on the pitching moment of the wing at the specified angle of attack, the tail volume coefficient, and the pitching moment caused by the A/C c.g. With Clt, the induced drag and form drag of the tail could be calculated. This was added to the form and induced drag of the wing, along with the Cdo of the fuselage.

$$C_D = C_{D0_f} + C_{D0_w} + C_{Di_w} + C_{D0_t} + C_{Di_t} \quad \textbf{EQN 9.3}$$

The lift force of the wing was calculated at design, which was added to the lift at the tail to find the total lift of the aircraft.

$$C_L = C_{L_W} + C_{L_t} \qquad \textbf{EQN 9.4}$$

The total lift of the aircraft was then divided by the total drag of the aircraft, giving the actual trimmed L/D of the CUAV Lemming. The team found that the resulting maximum L/D was 8.42, which shows the importance of including trim drag corrections in the calculation of the performance of an aircraft. Figure 11.3 shows this trimmed drag polar of the CUAV. With this the Aerodynamics Team was satisfied with their contribution to Lemming Team, and the design of the CUAV.

Chapter 10 Stability and Control

The cost minimization motif continued in the selection of tail surfaces. Minimization of the aircraft's cost lead the team away from a type of tail which would require two different surfaces to be constructed. If the Lemming team used a V tail with a symmetric airfoil only one type of wing would have to be manufactured, reducing cost. The team decided that this was more important, and stuck with the inverted V tail originally given to the concept. This type of V tail was favorable because it had proverse yaw response to rudder deflections. The size of the V tail was sized using Raymer's[10.1] control volume coefficients based on historical values. It was found that horizontal area of the tail was the driving factor in the sizing of the tail. This was partly due to the effort of the team to make the tail boom longer than the wing, to provide some protection to the one wing-tip during transport. This method found that a total area of 1.56ft^2 was required in planform area to create a stable aircraft. This was applied to a 45deg angle of anhedral, and a planform AR of 6 to find the actual tail span of 2.21ft per side, with a 6inch chord.

10.1 Method of Analysis

The stability and control of the CUAV was accomplished using several different codes. Initially, the program JKayVLM was used to evaluate each concepts neutral point. A chart of this analysis is available in Table 10.1

Table 10.1: Comparison of Preferred Concepts' Neutral Point

	Delta Wing	Convent-ional	DBF VLM	DBF - Actual	Error (%)
Cm_	-0.6166	-1.0655	-1.1127	-0.8950	24.3184
Cl_	2.4338	4.3764	6.8005	5.0500	34.6638
Cm_/Cl_	-0.2534	-0.2435	-0.1636	-0.1772	7.6797
H	0.2500	0.2500	0.2500	0.2500	0.0000
Neutral Point	0.5034	0.4935	0.4136	0.4272	3.1857

The lateral directional functionality of JKayVLM was not used to determine the aircraft's stability because it is known to have poor correlation. Instead the team used the Tornado VLM code to do a more complete analysis of the aircraft. This is because the Tornado code actually uses the slope of the camber line to determine the pitching moment of the wing, providing a more accurate answer. An attempt was made to validate the code using the pitching moment and lift curve slope produced by XFOIL with similar values produced by Tornado. The team found these values to be accurate. The CUAV was evaluated in one flight condition, the cruise condition.

10.2 Static Stability

The results from a central difference expansion in the Tornado code around the flight state of 0degrees AoA, and V = 135fps = 41.156m/s, provided the basic static stability derivatives of the CUAV aircraft. The neutral point of the aircraft was found to be at 52.97% of the Mean Aerodynamic Chord (MAC) during cruise flight. The maximum forward CG location was not determined by traditional methods. Since endurance is a driving factor in the design of the CUAV, minimizing trim loads is important. Figure 10.1 shows the required tail lift coefficient for each AoA for several different forward CG locations, they correspond to half-inch increments of the CG. An interesting thing to note is the hop in the required tail lift around 2 degrees AoA. This is directly correlated to a burble in the airfoil $C_{m\_}$ predicted by XFOIL. The team decided that the maximum deflection of the tail should not exceed half of the maximum C_l of the tail. This restricted the maximum C_l of the tail to 0.45, thus determining the maximum forward CG location at the 17.86% MAC location. This results in a total permissible CG shift of 4.92inches. Table 10.2 has the complete static stability parameters calculated thus far. All these values show that the CUAV is a stable aircraft, which is required by our flight control system.

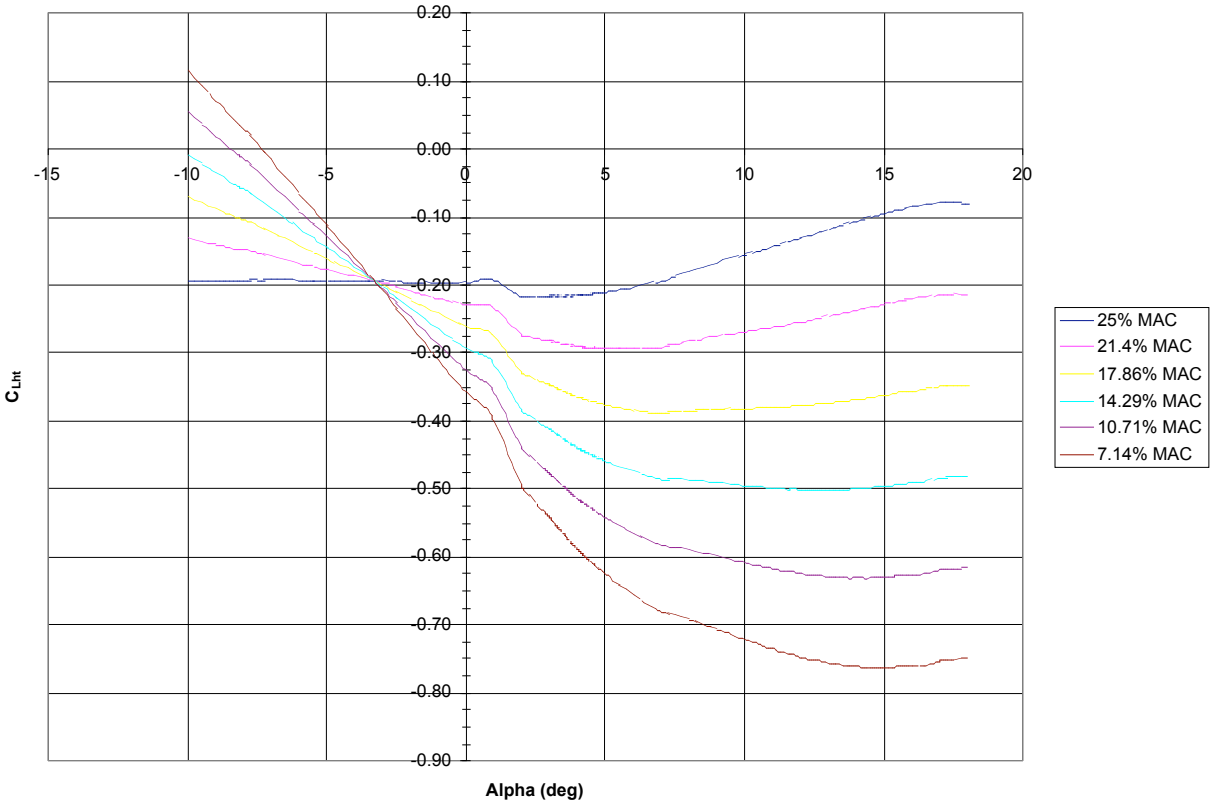

Figure 10.1: Tail lift coefficients for level flight

Table 10.2: Stability parameters for CUAV

	Longitudinal					Lateral-Directional			
Static	$C_{L\_}$	5.1404	$C_{m\_}$	-1.4376		C_l	0.0349	C_n	0.0130
Control Deflection			C_{m_E}	-2.7082		C_{l_A}	0.3145	C_{n_A}	-0.0193
		Static Margin		23.31%		C_{l_R}	0.0398	C_{n_R}	0.2168

Chapter 11 Materials

11.1 Discussion of Aluminium and Composite Construction

Team Lemming's material selection for the UAV was derived from an analysis of various materials. The two groups of materials that the team decided to focus on were Aluminum and Composites. Both materials are extremely popular in Aircraft industry due to their suitable qualities.

Aluminum is an abundant low cost material, with characteristics that make it perfect for our UAV construction. It is a versatile material with super corrosion resistance, good formability, flexibility, and strength.. Composites are often overlooked when cost is an important consideration. However, with such advanced characteristics, including great fatigue resistance, good damping characteristics, and very light weight they came out on top for best performance. In some cases this performance resulted in an actual cost saving.

The selection process required further analysis between both materials groups. The following is a list of the various aluminums and composites that had to be compared in order to select the most suitable from each category: Carbon Graphite (Unidirectional, Bi-directional Plain Weave, Bi-directional 8HS Weave); E-Glass Fibreglass (120, 3733, 7533), Bi-directional Kevlar; And Aluminium (2024T3, 7075T6, 6061T6).

In order to compare the materials, the thickness (in), cost ($/yd^2), tensile strength (lb/in) and weights (lb/yd^2) were recorded. Dividing the given value by the material thickness then normalized the cost. Next, a final score (X) was obtained for each material using Equation 9.1.

$$X = \frac{\text{Tensile Strength}}{\text{Cost} \cdot \text{Weight}} \qquad \textbf{EQN 9.1}$$

The optimal composite material and Aluminum alloys were selected. This is depicted in Figure 9.1 below.

Table 11.1: Comparison of Material Properties

Composite	t	cost	cost	weight	$?_{yield}$	score
	(in)	($/yd^2)	($/yd^2/in)	(oz/yd^2)	(lb/in)	
Uni Carb Graphite	0.006	14.76	2.46	4.70	550	47.570
Bi Carb Graphite (Plain)	0.007	16.48	2.35	5.70	300	22.356
Bi Carb Graphite (8HS)	0.013	27.44	2.11	10.90	650	28.252
120 E Fiberglass	0.004	4.80	1.20	3.08	125	33.820
3733 E Fiberglass	0.010	5.40	0.54	5.85	250	79.139
7533 E Fiberglass	0.009	5.70	0.63	5.64	250	69.989
Bidirectional Kevlar	0.010	14.50	1.45	5.00	630	86.897
Aluminum Alloy						Al score
2024T3	0.040	33.93	0.85	5.184	1880	427.532
6061T6	0.040	15.234	0.38	5.130	1400	716.567
7075T6	0.040	39.17	0.98	5.238	2920	569.277

After a detailed analysis of material it was decided that the best choice for our UAV was the use of Aluminum 6061T6 and the composite material Bi-directional Kevlar. Although cost is our driving factor in material consideration, there was not a large discrepancy between the cost of Aluminium construction and that of the Bi-directional Kevlar. Thus, it was found that the best choice for our UAV was the use of Bi directional Kevlar composite. Research presented in section 9.1 indicates that weight savings of up to 15% are possible with the use of composite construction. This weight difference will provide crucial savings in engine power and fuel consumption. Therefore, the determination was made that the UAV airframe will be constructed of a composite material. Referring again to Figure 9.1, the most efficient composite material for airframe construction is the Bi-directional Kevlar.

Bi directional composite consists of high strength fibres embedded in an epoxy matrix. These composites provide for major weight savings, up to 20%, while maintaining similar characteristics as Aluminium. Some of the advantages to composites are listed below:

- Low weight / low material density: composite densities range from 0.045 lb/in3 to 0.065 lb/in3 as compared to 0.10 lb/in3 for Aluminium
- Ability to tailor the fibre/resin mix to meet stiffness and strength requirements
- Elimination of part interfaces via composite moulding
- Low cost, high volume manufacturing methods
- Tapered Sections and Compound Contours Easily Accomplished
- High resistance to corrosion
- Resistance to fatigue
- High Damping Characteristics
- Low coefficient of thermal expansion

Composites possess inherent properties that provide performance benefits over metals. A wide range of fibres and resins are available for the selection of the optimal material combination. The high strength-to-weight and stiffness-to-weight ratios are the primary reasons composites are widely used. In addition, all metal castings contain notches that can catastrophically fracture under impact due to their respective stress concentrations. The fibre reinforcement of composites alters this failure sequence resulting in an increased resistance to impact. The impact toughness of composites can be maximized by fibre selection, length of fibre and use of tougher resin such as thermoplastics.

By using Bi directional Kevlar we will greatly reduce weight and advance in performance using a composite for our construction can also provide a consolidation of parts, thus improving the reliability of the structure and keeping the costs competitive with metallic structure.

The team initially decided to completely construct our UAV of composite material, which would mainly be 0.03" thick with slight variations throughout to compensate for any high stress concentrations present due to internal loading.

In order to gain a more thorough understanding into where the thickness may vary the UAV frame and its loads were analyzed in a finite-element stress-analysis program. It was found from this analysis that the applied loads on the frame caused slight deformation. In order to avoid any kind of joint separation or buckling the team decided it was best to reinforce the structure with aluminum beams.

As well as increasing our safety factor this choice also forced out any possibility of stress failure, and proved cheaper than using thickness variation on the Kevlar. The weight of the additional Aluminum frame was not of any concern as the team was still well under the initial estimate of the weight provided in the preliminary design.

Chapter 12 Structures

12.1 Load Analysis of Wing

To begin the structural analysis of our UAV design the wing loading was examined for straight and level flight as well as a 3-g turn. By estimating a wing loading the shear force and the bending moment could be determined for the design. Knowing the shear force and bending moments in the wings

of the UAV played a key role in the overall design of the internals of the wing. These values helped determine the required thickness of the wing, spar sizing, and on the final material selection for the wings. In order to perform these calculations some assumptions had to be made. First, it was assumed that the wings would have an elliptical loading where the lift would be equal to the weight of the aircraft. The lift along the wing of the UAV was estimated using equation 12.1:

$$F(x) = L_{root}\sqrt{2 * x * length - \left(\frac{x}{length}\right)^2} \quad \textbf{EQN: 12.1}$$

For this equation L_{root} represented the lift on the wing at the fuselage and was determined so that the total lift was equal to the weight of the aircraft. The other assumption made during these calculations was that the wing would weigh 12 lbs for the spar weight and the skin weight. From the wing weight and the elliptical lift loading, the wing loading could then be determined as a function of the wingspan. The shear force in the wing was then determined by integrating the wing loading. From the shear force the bending moment in the wing could then be calculated by integrating the shear. To determine the max values of shear force and bending moment the determined equations were then evaluated at the wing root, next to the fuselage.

To perform the structural analysis on our UAV designs a Matlab code was written to perform the necessary calculations for the wing loading and the integrations to determine the shear force and the bending moment. The wing loading, shear, and bending moment were then all plotted as a function of the wingspan. For the conventional design a total weight of 187lbs and a wingspan of 10 ft were used in the calculations. For each of these plots the wing root is located at the origin and the wing tip is located at the maximum value of the length along the x-axis (Figure 12.1). From these values it was determined that the conventional UAV design would have a maximum shear force of 81.50 lbs (Figure 12.2) and a maximum bending moment of 168.41 ft-lbs (Figure 12.3) located at the root.

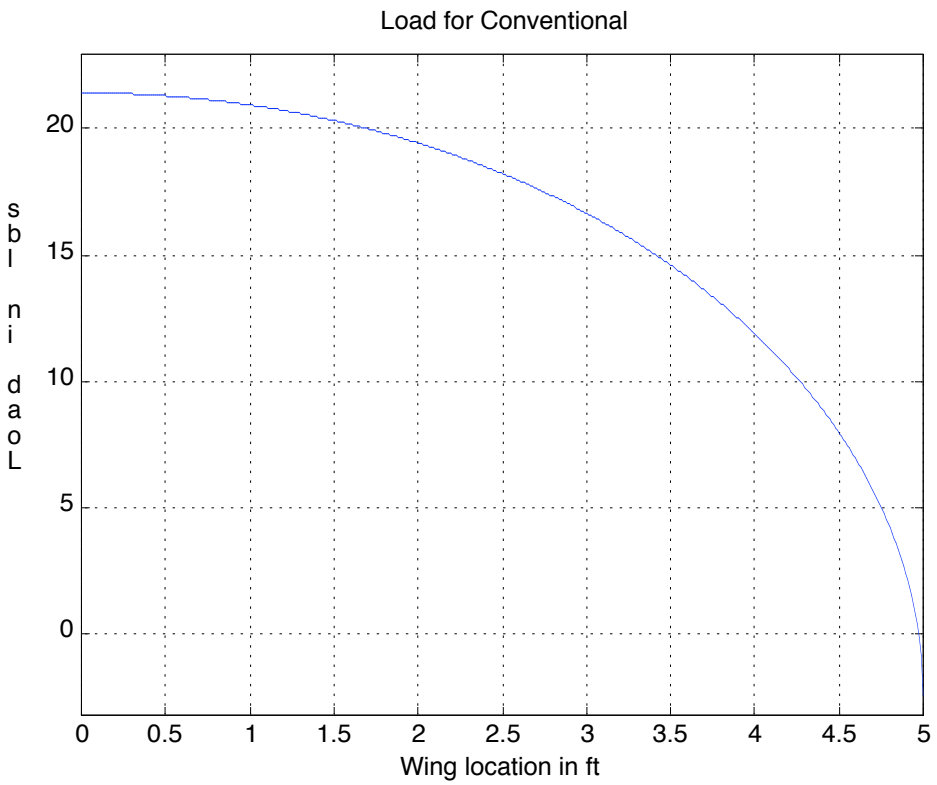

Figure 12.1: Wing loading for straight and level flight

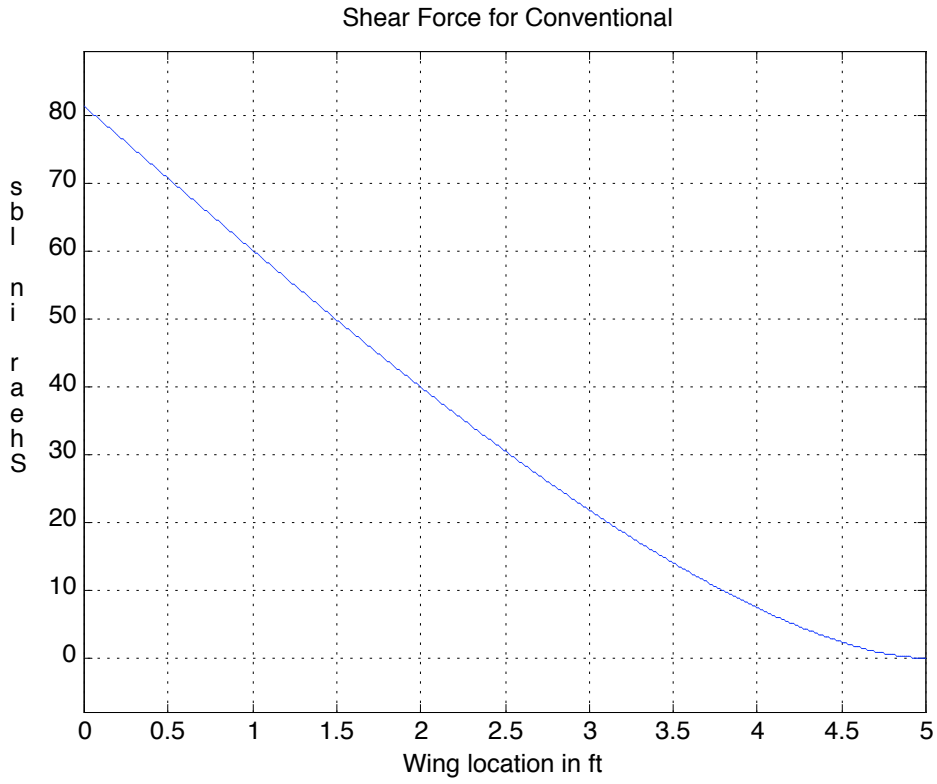

Figure 12.2: Shear force for straight and level flight

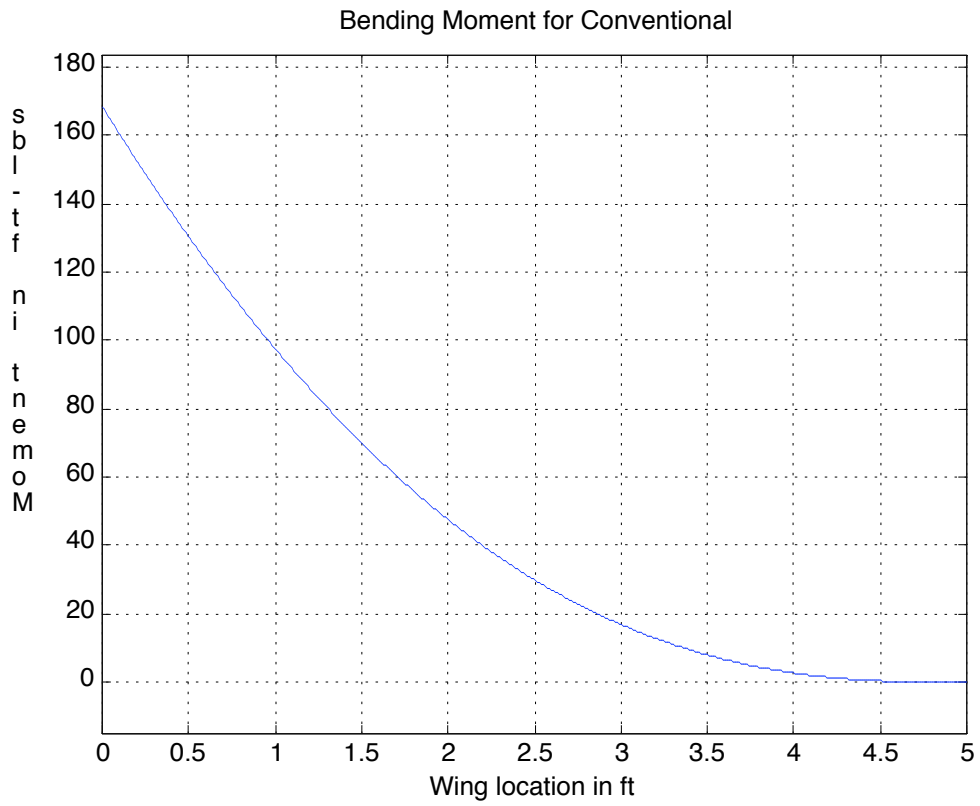

Figure 12.3: Bending moment for straight and level flight

To continue on with the structural aspect of the cheap UAV design, the V-n diagram was constructed. The V-n diagram would provide useful information on the maneuver loading as well as the gust load conditions. It was decided that the UAV would be capable of a maximum loading of 3-g's and a minimum loading of –1.2-g's. To construct the V-n diagrams a Matlab script was written to construct three diagrams, a maneuver diagram, a gusting diagram, and a combination diagram. The basic equation[12.1] for the maneuver diagram construction can be seen below:

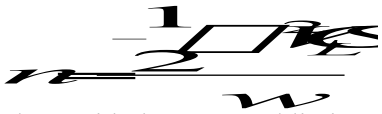

EQN 12.2

Using this equation along with the structural limits and the maximum velocity the maneuver V-n diagram was constructed (Figure 12.4).

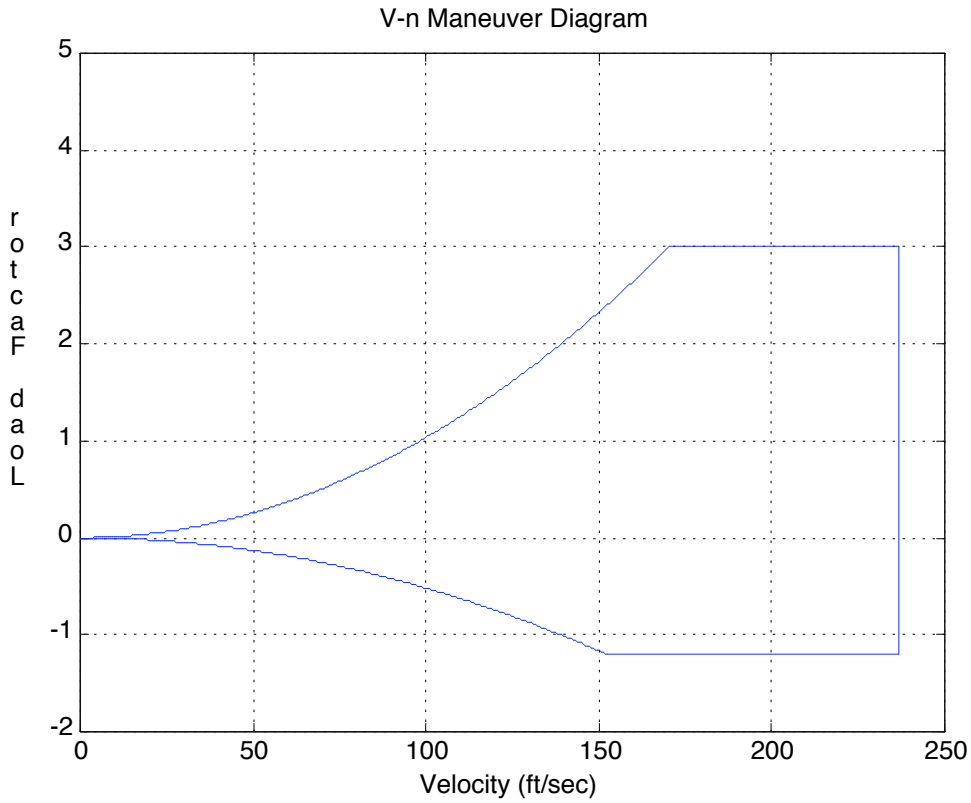

Figure 12.4: Maneuver V-n diagram for cheap UAV

The next phase of the V-n diagram was to construct the gust diagram. Values for gusting conditions are up drafts, which in a sense change the angle of attack of the aircraft due to the change in free stream direction. These sudden changes in loading can often cause control problems as well as structural problems. The gusting conditions for the UAV are 66 ft/sec at stall, 50 ft/sec at cruise, and 25 ft/sec at maximum velocity[12.2]. The governing equations[12.1 and 12.2] for the gust loading calculations can be seen below:

$$\mu = \frac{2W}{\rho c a g s} \qquad \textbf{EQN 12.3}$$

$$K_g = \frac{0.88\mu}{5.3 + \mu} \qquad \textbf{EQN 12.4}$$

$$n = 1 + \frac{K_g V_e a U_{de}}{498 \frac{W}{S}} \qquad \textbf{EQN 12.5}$$

Using these three equations along with the different gust velocities the gusting diagram was constructed by a Matlab scripts (Figure 12.5). By combing the maneuver V-n diagram and the gusting diagram it is possible to determine the possible effects gusting will have on the structural aspect of the design. Using a Matlab script a combination V-n diagram was constructed to compare the gusting and maneuver diagrams (Figure 12.6). From this V-n diagram it can be seen that the UAV can't be structurally damaged by an updraft, but the updraft will cause the UAV to stall. At points past the stall line and maximum structure loading intersection, the gust loading conditions are all well inside of the maneuver diagram.

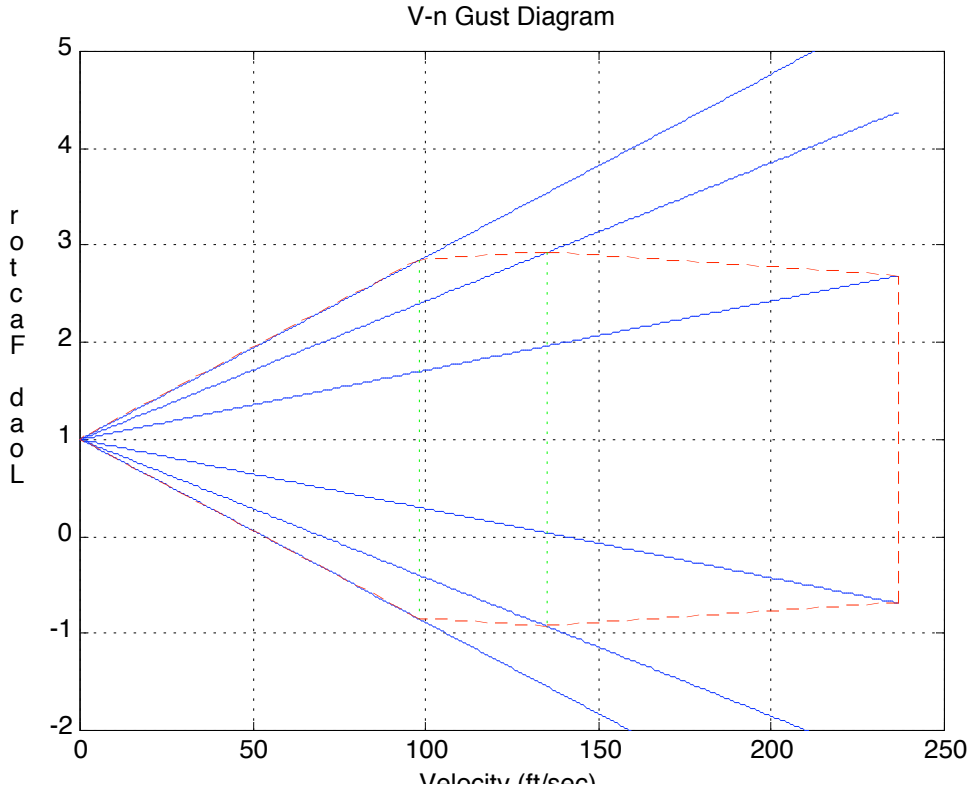

Figure 12.5: Gusting V-n diagram for CUAV. Blue lines represent gust lines for the three gust conditions. Red lines represent the gust loading. Green lines show the stall and cruise speed.

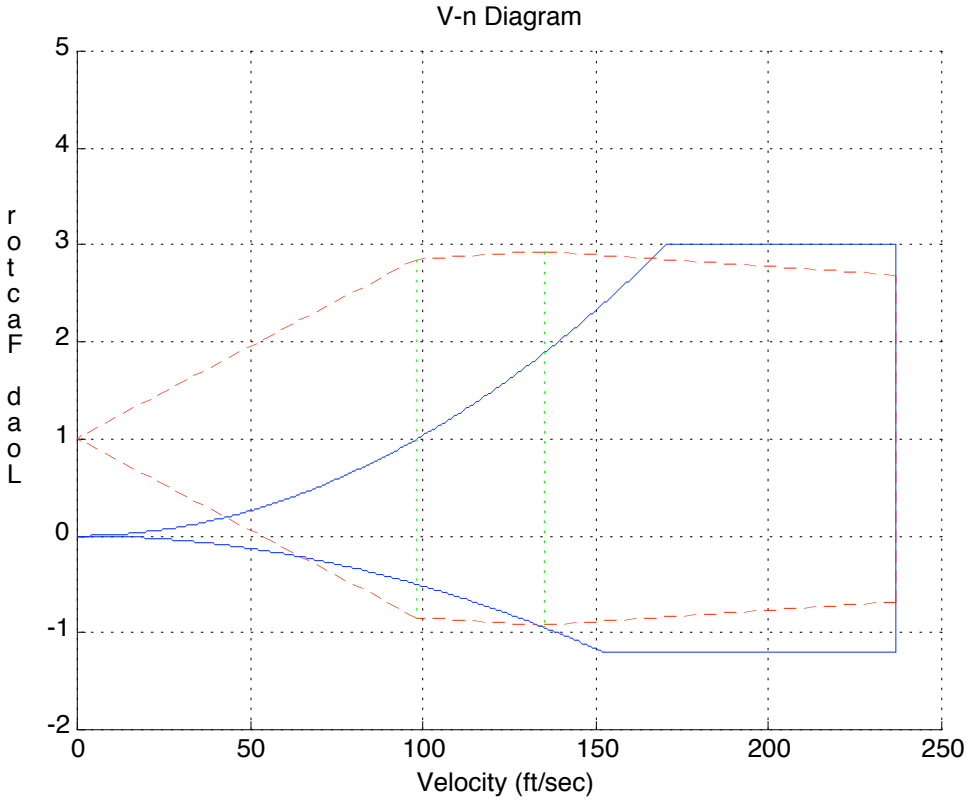

Figure 12.6: V-n diagram for cheap UAV. Blue lines show maneuver, red lines show gusting, and green lines represent stall and cruise speed

12.2 Wing and Tail Spar Design

The next phase of the structure design of the cheap UAV was the spar designs for both the wings and the tails. In both cases C-beams would be used for simplicity to reduce the cost of manufacturing. The wing was designed to have two C-beams located in the wing, one around the quarter chord and another back around 75% of the chord. It was decided to try and use the same size C-beam for both the front and back of the wing to reduce cost. Using the same size beam had its disadvantage though, due to the size requirements the rear beam couldn't be placed as far back as desired for the aileron integration so a hinge system would have to be developed later. The C-beams were sized using a Matlab script that accounted for the beams maximum shearing force, compression due to bending, and deflection of the wing. The following equations[12.3] were used in the constructed Matlab script to inure the spars would not fail:

$$\sigma = \frac{Mc}{I_x} \qquad \textbf{EQN 12.6}$$

$$\tau = \frac{VQ}{It} \qquad \textbf{EQN 12.7}$$

$$\frac{d^2y}{dx^2} = \frac{M}{EI}$$ **EQN 12.8**

Using these equations to determine the maneuver shearing force, compressive stress, and beam deflection along with the yield strength of the 6061t6 aluminum the spars could be properly sized. Using the dimensions of the midnight airfoil for the wing, it was decided to place the front spar at the 20% chord and that the rear spar location would be moved as far back as possible. To account for the skin thickness the wing spar was given a height of 1.54 inches. The spar thickness was set to be 0.1 inches and then the spar width was adjusted until the spar did not fail any of the three requirements. As it turned out, the sizing factor for the spar width was the compressive stress due to bending. Using a width of 0.6 inches for the spar gave a satisfactory spar design with a small factor of safety. The yield strength of the 6061t6 aluminum in compression was 35,000 psi[12.4] and the spar design has a compressive stress of 32,800 psi. For the rear spar, the location was determined based on the geometry of the spar and of the airfoil. Accounting for the skin thickness it was determined that the rear spar would be located at 56% of the chord. From this it was determined that a hinge attachment would be

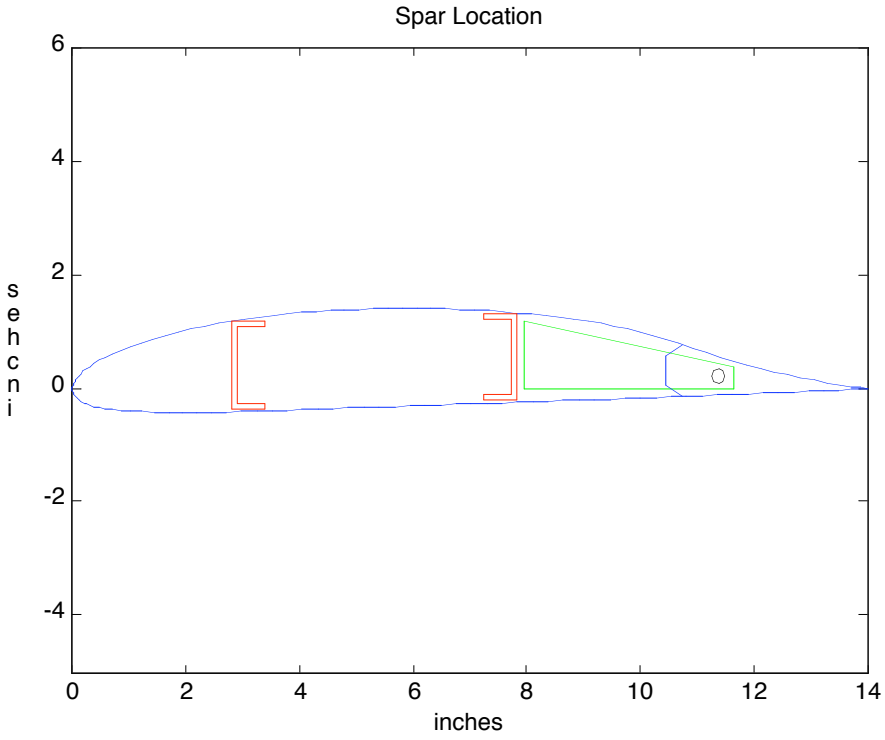

Figure 12.7: Midnight airfoil with spar locations and hinge attachment for wings

required to move the location of the hinge for the ailerons back to 75% of the chord instead of 56% of the chord. From the Matlab script that was used to determine the spar locations a diagram of the midnight airfoil and the spar locations was constructed (Figure 12.7). This C-beam design produced a total beam weight of 6.03 lbs.

To move the location of the hinge for the ailerons back two plates were designed to attach to the rear spar at each end of the ailerons. The attachments were designed to have having a minimum thickness of 0.1 inches and a 0.25 inch diameter hole for the aileron attachment. The aileron attachment was set at the quarter chord of the aileron to reduce the moment on it, which would reduce flutter. This set the center of the hole for the attachment 3.45 inches back from the rear of the spar. The design was checked to insure it would not fail due to shearing stress around the hole used for attaching the aileron. The locations of the spar attachments can be seen in Figure 12.8, which was developed in Unigraphics.

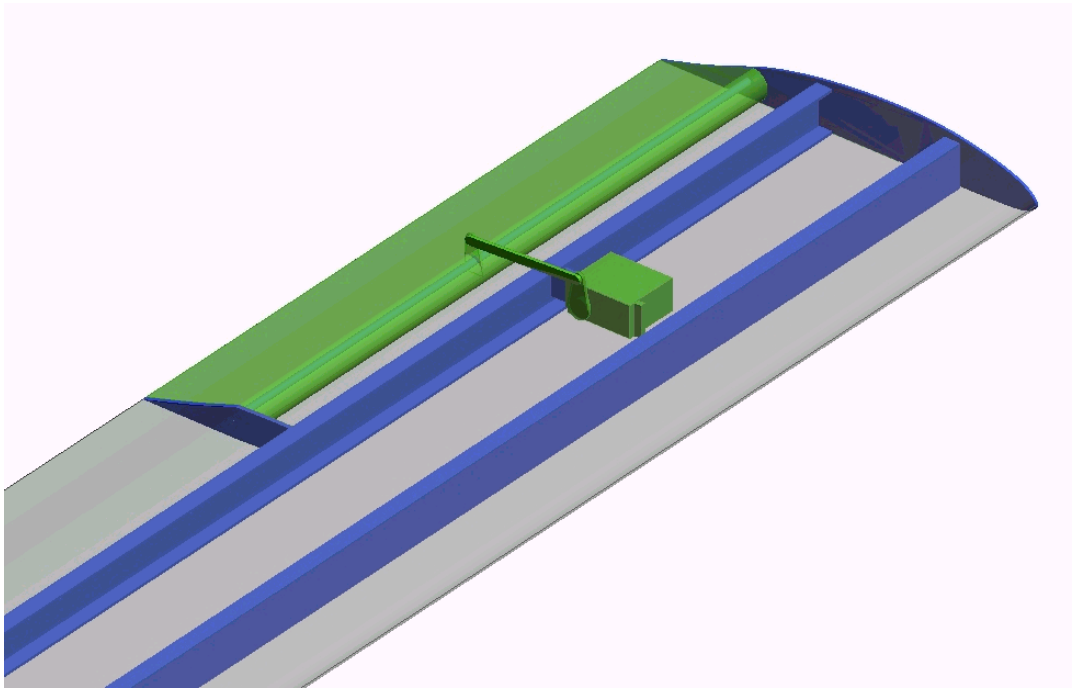

Figure 12.8: Spar attachments for aileron integration

For the tail spar sizing a similar Matlab code to the one for the wing spar sizing was developed. The spar for the tail would be a single C-beam located at the quarter chord. The Height of the beam was once again determined by the airfoil size. In this case, the airfoil was a NACA 0009 airfoil. Accounting for the skin thickness this produced a spar height of 0.50 inches. Using the same sizing parameter as before and a beam thickness of 0.1 inches the beam width could be determined. The loading for the tail was determined to be the loading required for a 3-g turn. Using this loading it was determined that the beam deflection would be the driving factor in the width sizing. Using a beam deflection of 5% of the length of the tail, it was determined that a width of 0.4 inches would be required. Using the airfoil dimensions and the spar size, a diagram of the spar location was constructed (Figure 12.9).

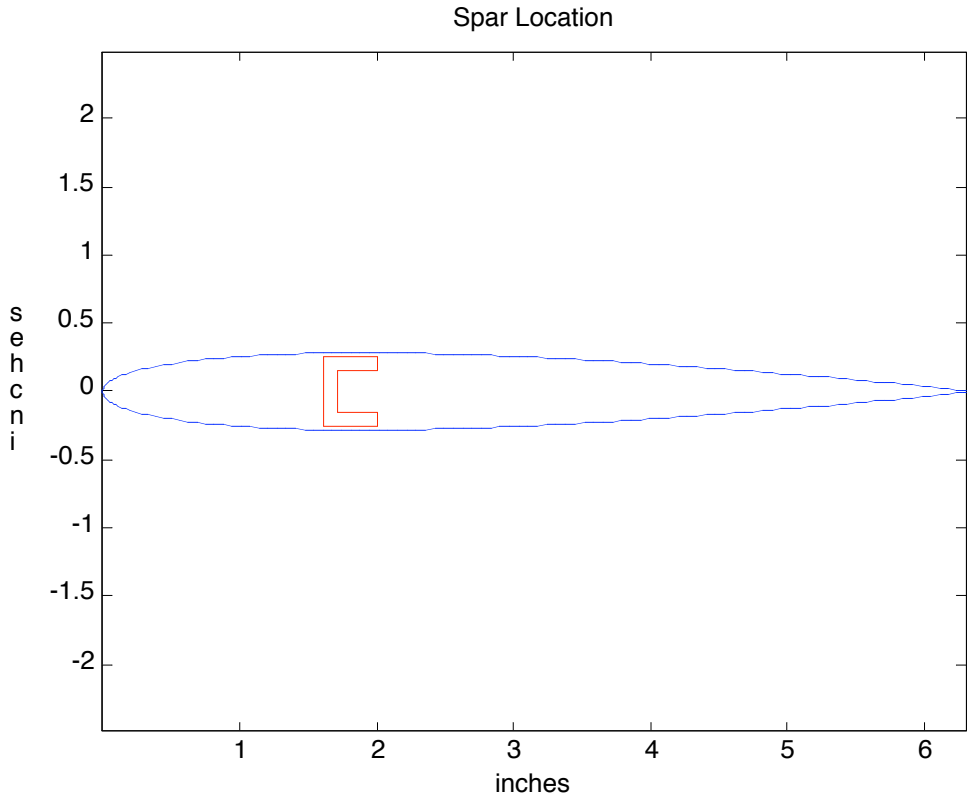

Figure 12.9: NACA 0009 airfoil with spar locations for tail

To attach the tails to the boom of the UAV a bearing system was developed. Since the tail was to be full flying the attachment directly linked to the spars in the tails. A rod was placed inside of the spars of the tails and extended out into the boom of the UAV. The rod was attached to the UAV by two

bearings, which could be rotated by the servos located in the fuselage of the UAV. To accomplish this integration one of the tails had to be moved back slightly so that the two rods from the tails would not interfere with each other. The layout for this design can be seen in Figure 12.10, which was developed in Unigraphics.

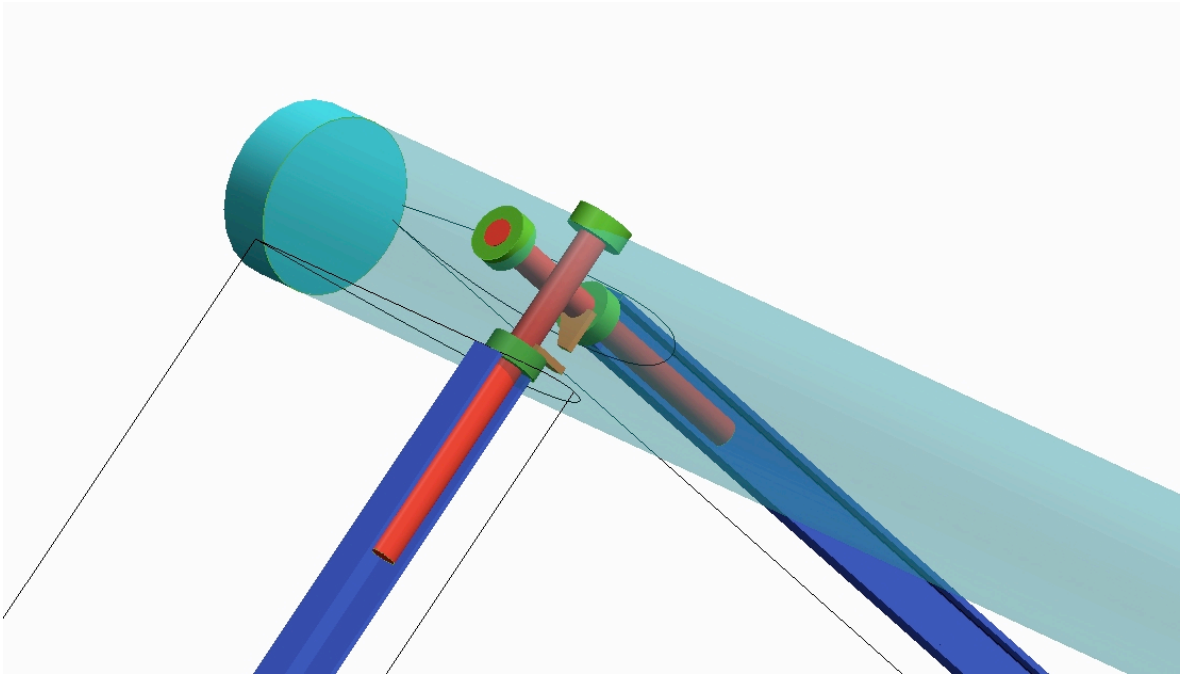

Figure 12.10: Tail integration into boom of UAV

Chapter 13 – Weights, CG, and Moments of Inertia

13.1 Method Used

In order to calculate the weight, center of gravity, and second area moments of inertia of Team Lemming's UAV, a program was developed in MATLAB. The program, called "UAVwtcg," is executed from the MATLAB command window, and optionally accepts the fraction of fuel remaining in the fuel tank at which the calculations are to be performed. The program was written based on a completely "broken down" UAV, meaning that the aircraft must be broken down into 26 separate components. More specifically, six of the components are exterior skin components, 11 are airframe structural components, 2 are the nose cone and propeller, and the remaining components are interior features such as the engine,

fuel tank, batteries, payload, etc. A schematic diagram of this breakdown is shown in figure 13.1. In the diagram, the six fuselage skin components are labeled in green, and all 26 components are indicated with the red "point load" arrows. This demonstrates the fact that in the program, all components are treated as a point load at a certain longitudinal location.

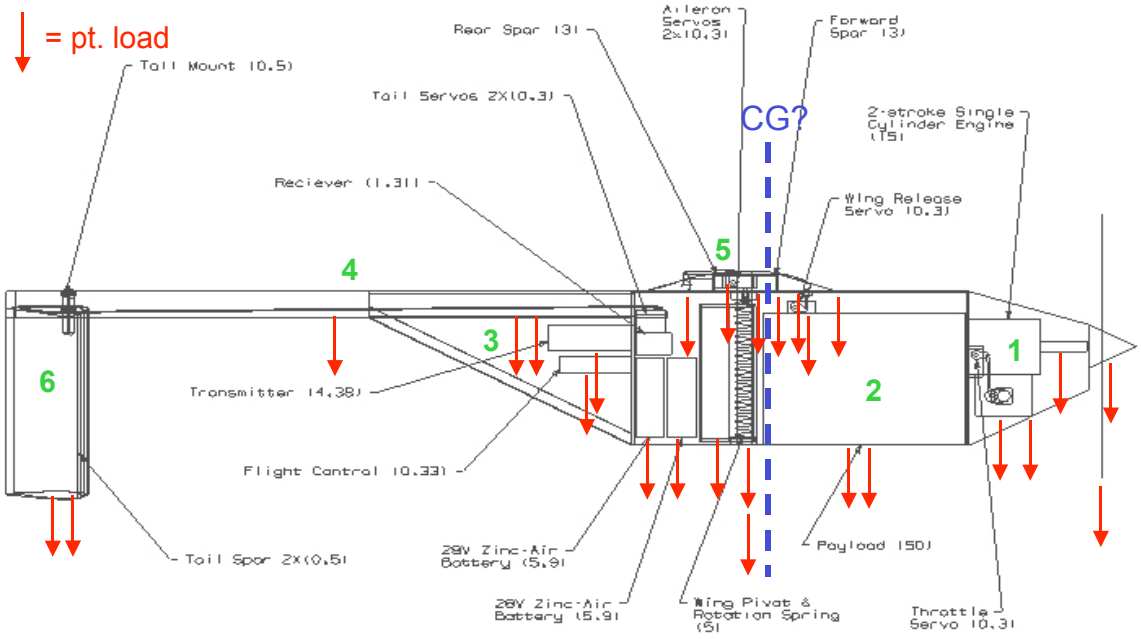

Figure 13.1: Component breakdown of UAV for weight calculation.

The program works by reading a data file with all of the necessary component dimensions, weights, locations, materials, etc. This data file can be manipulated and saved to allow for changes as the development of the UAV progresses. For all external components, this data includes the dimensions, the location (with respect to the nose of the UAV), the skin thickness, and the material used (Aluminum or Kevlar). For the wing and tail airfoils, the program asks the user for the cross-sectional x- and y-coordinates (as output by an aerodynamics program). This is the only user-supplied input. It should be noted that the densities of the materials are hard coded, and also that a loop is executed for each airfoil, calculating their perimeters and volumes using the Pythagorean Theorem. The weight of each external component and the local cg's are then calculated using geometry. For the internal components, the data file supplies the program with the weights and local centers of gravity of each.

When executed, the program proceeds through each of the 26 components, calculating the total weight and local CG of each component for which such data is not already supplied by the data file. The program then calculates the Kevlar skin weight and the Aluminum airframe weight, so as to provide a basis for material cost considerations. Next, the weight of the entire UAV is calculated by summing the individual component weights. All of these numbers are displayed to the user, as well as the individual weights of each component.

Next, the calculation of the center of gravity of the UAV is performed. To do this, the moments created by the displacement from the overall CG of each point load were summed using equation 13.1. In other words, each component weight was multiplied by its distance from the unknown center of gravity. At the center of gravity, the sum of all of these moments must equal zero. This provides one equation, with one unknown:

$$\sum M_{cg} = 0 = \sum [weight_i * (localcg_i - cg)] \qquad \textbf{EQN 13.1}$$

To find the cg from this equation, the program performs matrix arithmetic. Once the CG is calculated, it is displayed to the user, along with the individual component CG's.

The next step performed by UAVwtcg is the calculation of the second area moments of inertia, for stability purposes. Two moments of inertia were determined: the pitch moment of inertia (I_{xx}), and the roll moment of inertia (I_{yy}). To calculate I_{xx}, the Parallel Axis Theorem was used (eq. 13.2):

$$I_{xx,total} = \sum [I_{xx,local} + Ad^2]_i; \qquad \textbf{EQN 13.2}$$

where $I_{xx,local}$ is the local area moment of inertia, A is the cross-sectional area of the entity under consideration, and d is the distance from the local cg to the UAV cg. The total I_{xx} of the UAV is calculated simply by summing the individual moments of inertia of each component. The program uses the component dimensions previously supplied by the user to perform these calculations.

Because all of the UAV's components are laterally centered on the aircraft's longitudinal midline, the Parallel Axis Theorem is not needed. The local second area moments of inertia are calculated and summed to obtain the UAV roll moment of inertia. Both I_{xx} and I_{yy} are displayed to the user, and carry the dimension of: inches^4. Figure 13.2 depicts sample snapshots of the output produced by UAVwtcg:

13.2 Results

The values produced by the execution of UAVwtcg are shown in Table 13.1, below. The results shown were obtained using a universal skin thickness of 0.06", using Bi-Directional Kevlar. Also, the fuel tank was assumed to be full.

Table 13.1: UAV properties (results of UAVwtcg).

Skin Weight	**10.61**	**lb**
Airframe Weight	**36.07**	**lb**
UAV Weight	**159.39**	**lb**
UAV CG fm shaft	**0.57**	**in**
I_{xx}	**216129**	**in^4**
I_{yy}	**759934**	**in^4**

The most important value shown here is the location of the center of gravity of the UAV. It is desired that the CG be as close to the wing center of lift, or the vertical shaft in fuselage section 2, as possible. These results indicate that the center of gravity is 0.57" forward of the shaft with a full fuel tank and 50 lb payload.

In addition, the influence of varying the fuel amount and payload weight was studied. Figure 13.3 shows three plots of the UAV CG location as a function of the payload weight (from 20 to 50 lb) with the red line, for two fuel amounts: 100%, and 5% (full and empty). The black horizontal line indicates the location of the spring and shaft to which the wing is attached.

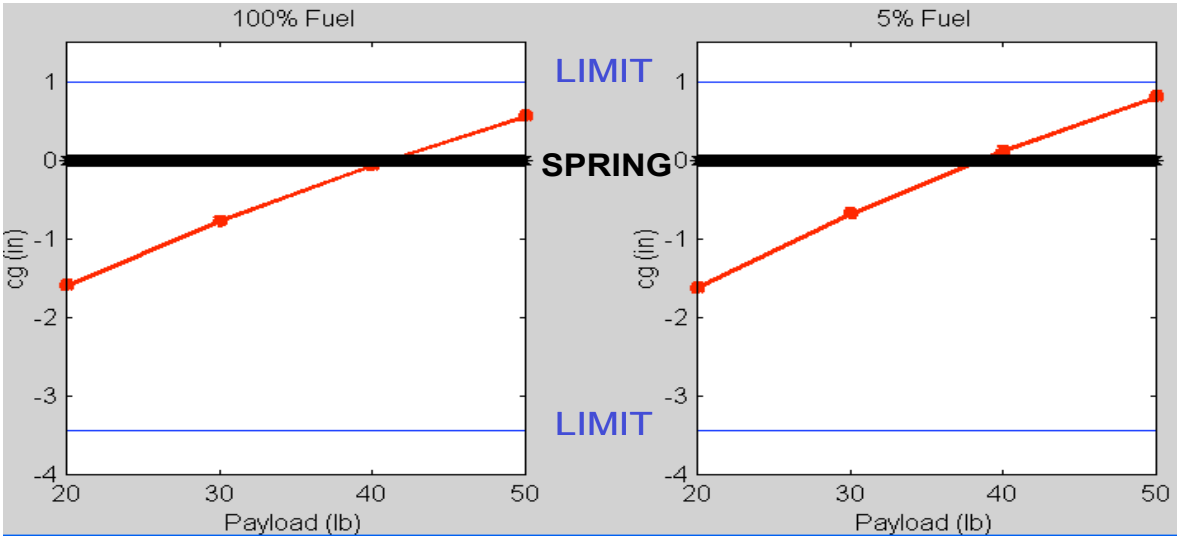

Figure 13.2: UAV CG location as a function of fuel and payload.

From the plots, it can be seen that for all reasonable payload weights, the center of gravity remains in the acceptable region. The acceptable region was defined by previous stability and control calculations. For this aircraft, the endpoints of this region are the neutral point, or 49.35% chord (3.433" behind shaft), and one inch forward of the shaft. These limits are indicated on the plots by the blue horizontal lines.

Chapter 14 Systems

14.1 Systems Overview

For satisfactory completion of the CUAV reconnaissance mission, several systems had to be integrated into the CUAV design. These systems include; communication and control, autopilot and navigation, control actuation, electrical, fuel, wing articulation, and deployment integration systems. For each of these systems, the group developed basic requirements and researched existing systems to fulfill the design requirements. From the existing products found suitable for the project, systems were chosen largely on merit of cost. The following sections will discuss each of these systems in detail.

14.2 Communication System

The communication system is one of the most important systems in a reconnaissance UAV. If the UAV is unable to convey the reconnaissance information to the base station or accept command

inputs, then the craft is unable to perform its mission. Consequently, considerable research was put into selection of a communication system.

The Lemming philosophy for the CUAV data link is to utilize existing ground, ship and aerial based control stations for control of the CUAV. Consequently, if operated by the US Navy, the CUAV would use the Pioneer system control stations. If operated by the US army, the control stations built by AAI Corporation for the Shadow systems would be used. In this way, the Lemming group avoids the research and development cost of creating a new control system. Furthermore, this decision makes the CUAV a more attractive product to the Navy because they only have to buy the air vehicle itself and can use their existing hardware for control, thereby saving money and training time.

The original requirements for the aerial data link were as follows; the link must accept flight control inputs from the ground station, transmit flight telemetry and reconnaissance information possibly including a real time video feed, and the link should have a range of 100 miles.

Figure 14.1: Tactical Common Data Link

The first data link considered for the CUAV was a Tactical Common Data Link (TCDL). The TCDL is a microwave communication system protocol developed by the Department of Defense in 1991 to standardize all US tactical reconnaissance transmissions. TCDL systems are utilized on most tactical UAVs used by the US military, including the Shadow, Predator, and Pioneer systems. The components of a TCDL system are shown in figure 14.1.

Because these systems are the current military standard, the group originally intended to use a TCDL for the aerial data link to better facilitate the use of existing control stations. However, the cost of a Tactical Common Data Link was found to be prohibitively high for use in the CUAV. L3 Communications, a leading manufacturer of TCDL systems, quoted aerial data link prices of $200,000 and up [14.1]. Since this cost is 10 times the target fly-away cost of the CUAV, an alternative data link had to be found.

The group sent emails to several wireless communications companies asking for quotes on aerial data links suitable for our mission. Three companies gave favorable responses; AACOM Systems, VTEX Communications, and Spectralink Communications. Each company described a system suitable for our reconnaissance mission with a line of sight range of roughly 50 miles. All three companies indicated that such a system could be purchased for roughly $15,000. The AACOM system was chosen for the CUAV because of the fact that they were the only company based in the United States. The specific configuration of the data link is based on the highly informative emails sent by Mr. Bruce Hobbs [14.2] of AACOM.

A summary of the data link specifications can be seen in table 14.1. Data link integration into the CUAV design can be seen in figure 14.5.

Table 14.1: Summary of aerial data link specifications

Data Link Specifications			
AACOM AT6420 Transmitter		AACOM 3000 Receiver	
Range	50 miles	Range	50 miles
Voltage Input	28 V DC	Voltage Input	28 V DC
Current Draw	6.0 Amps	Current Draw	0.20 Amps
Dimensions	7" x 4.5" x 2.34"	Dimensions	3" x 4" x 1.95"
Weight	4.375 lbs	Weight	1.31 lbs
Power Output	20 Watt		
Antenna	20" Omni-directional colinear array		
Total Unit Cost	$15,000		

14.3 Autopilot and Navigation

For the autopilot and navigation systems on the CUAV, the team was able to exploit the expendable nature of the craft to reduce cost. Since the CUVA is not required to autonomously land, the craft does not require the accuracy in positioning, heading, or altitude currently found in existing military UAVs. Consequently, the team was able to utilize a far less sophisticated autopilot system.

The Autopilot system used in the CUAV is the Micropilot MP1000SYS autopilot [14.3]. This autopilot was originally designed to be used with model airplanes. The system consists of three main components. A stability and control computer, a navigation and mission control computer, and an integrated GPS antenna.

The stability computer controls the altitude, airspeed, airplane orientation, and heading of the UAV. "The stability computer uses the rudder to turn, the throttle maintains altitude, and the elevator maintains airspeed. Each of these flight parameters is sensed by an array of onboard sensors consisting of two rate gyros, a gravimetric accelerometer, a barometric pressure sensor and a Pitot style airspeed indicator."[14.3]

The navigation and mission control computer interfaces with the data link and GPS to determine course corrections, execute mission procedures, and respond to ground control inputs. The navigation computer is designed to operate in either an autonomous mode, or in an operator-controlled fashion. The controller chooses the choice of UAV mode or operator-controlled mode. However, if link contact is lost, the UAV can be programmed to automatically return to base. The navigation computer allows for uploading of waypoints before or during the mission. Waypoints can include altitude, airspeed, and mission function information.

The third unit is an integrated GPS receiver and antenna. The GPS receiver has a listed accuracy of ± 25 ft. The included antenna is 48 inches long. In the CUAV project, this antenna will be positioned in the tail boom of the craft, unless it is found that the aluminum tail boom interferes with the GPS reception.

There are two drawbacks inherent with the MP1000SYS autopilot, which the group deemed acceptable for the CUAV. In its commercial configuration, the autopilot is only able to control statically stable aircraft. This is not a problem since the CUAV will be designed for stability in all flight regimes to simplify autonomous control. Secondly, while the autopilot does support catapult launching of the craft, new codes would need to be written for the aerial deployment of the CUAV. However, without additional programming, the autopilot would work in the commercial state, as long as the craft is piloted manually during the launch procedure.

The specifications of the MP1000SYS autopilot are given in table 14.2. The MP1000SYS is shown in figure 14.2. The positioning of the unit in the UAV is shown in figure 14.5.

Table 14.2: Summary of autopilot specifications

Micropilot MP1000SYS Specifications	
GPS Accuracy	± 25 ft
Altitude Accuracy	± 5 ft
Speed Limit	255 fps
Altitude Limit	25,000 ft
Dimensions	6" x 3.2" x 1.5“
Weight	0.33 lbs
Antenna Length	48 in
Current Draw	0.30 Amps @ 8 V
Unit Cost	$2,000

Figure 14.2: Micropilot MP1000SYS

14.4 Control Actuation

From the onset of the design of the CUVA project, one of the suggested cost saving methods was to use model airplane servos for control actuation. Our choice of an autopilot system specifically designed to interface with model airplane servos made the use of these servos the logical choice, given their low cost and wide range of performance specifications. The only concern to the team with these servos was whether or not they could produce the necessary hinge moments for control actuation. From the aerodynamic analysis of the control surfaces, it was found that the hinge moments needed for flight were in the range from 0.24 – 0.34 ft-lbs. These torque values were found to be well within the design torques of _ scale model airplane servos. Consequently, the CUAV design utilizes these servos for actuation of the control surfaces and throttle control.

The placement of the servos in the CUAV is shown in figure 14.5**.** As shown in the figure 14.5, 1 servo is used for actuation of each control surface, and one servo is mounted on the firewall to control the throttle. Figure 14.3 shows a representative _ scale model airplane servo. Table 14.3 gives the specifications of these servos.

Table 14.3: Summary of _ scale servo specifications

1/4 Scale RC Servo Specifications	
Dimensions	2.33" x 1.13" x 1.96"
Torque	0.66 ft-lb -- 1.52 ft-lb
Avg Current	97 mA -- 495 mA
Unit Cost	$27.99 -- $94.99

Figure 14.3: _ Sale model airplane servo

14.5 Electrical System

There are two traditional methods for providing electrical power to a UAV. The first method is to simply carry enough batteries onboard to power all the UAV electronics. The second method is a combination of a base battery pack and a generator integrated with the UAV engine, provided the UAV does not use electric propulsion.

The team's choice of a go-kart engine to power the CUAV made the integration of an electric generator into the design effectively infeasible. Since the engine was never designed to accept a generator, attaching one would require considerable modification at great cost.

To evaluate battery systems, it was necessary to determine the total amount of electrical power the CUAV would require. Using the manufacturer's stated maximum current draw for each unit and assuming an average current draw for each servo based on reference 14.4, the required electrical power for the CUAV was calculated for a flight of 5.5 hours. The results, shown in table 14.4, indicate a required battery capacity of 110 Amp-hours. As shown in the table, this analysis assumes a payload current draw of 10 amps. If the payload requires more amperage, additional battery packs can be included as part of the 50 lb payload weight.

Table 14.4: CUAV electrical requirements

UAV Electrical Requirements	
System	**Amps**
Autopilot	0.30
Servos (times 5)	0.50
Reciever	0.20
Transmitter	6.00
Payload	10.00
Miscellaneous	1.00
Total	**20.00**
20 Amps x 5.5 hrs = 110 Ah	

Two different battery systems were considered for the CUAV; Lithium-Ion batteries, and Zinc-Air batteries. Lithium-Ion batteries are currently used in many military communication devices, and

Zinc-Air batteries have been developed to replace these battery packs. Radio-Recon distributor in Roanoke was contacted for specifications and pricing information on the Ultra-Life brand of Lithium-Ion batteries[14.5]. The Electric Fuel Corporation was contacted for information on the Zinc-Air batteries[14.6]. The comparison of the batteries is shown in table 14.5.

Table 14.5: Comparison of battery systems for the CUAV project

UAV Battery Selection						
Type	**Manufacturer**	**Voltage**	**Capacity**	**Weight**	**Dimensions**	**Cost**
Lithium-Ion	Ultra-Life	28 V	11 Ah	2.9 lb	5"x4.4"x2.45"	$125
Zinc - Air	Electric Fuel	28 V	56 Ah	5.9 lb	12.2"x7.3"x2.4"	$290
Zinc - Air	Electric Fuel	28 V	30 Ah	3.1 lb	12.2"x3.7"x2.7"	$210

Table 14.5 shows that the Zinc-Air batteries have an advantage in weight as well and price over the Lithium-Ion batteries. It would take 10 lithium batteries at a weight of 29 lbs and cost of $1,250 dollars to provide the required 110 Amp-hours. However, it would only take 2 of the 56 Ah zinc batteries to power the UAV at a weight of 11.8 lbs and cost of $580. Consequently, the decision to use Zinc-Air batteries was obvious.

The placement of the battery packs in the CUVA is shown in figure 14.5. A picture of the battery pack is shown in figure 14.4.

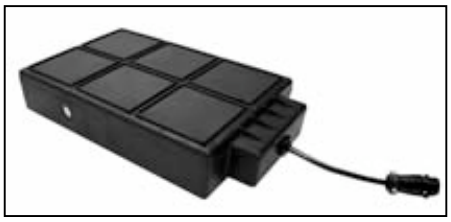

www.electricfuel.com

Figure 14.4: Electric Fuel Zinc-Air BA-8180/U battery pack

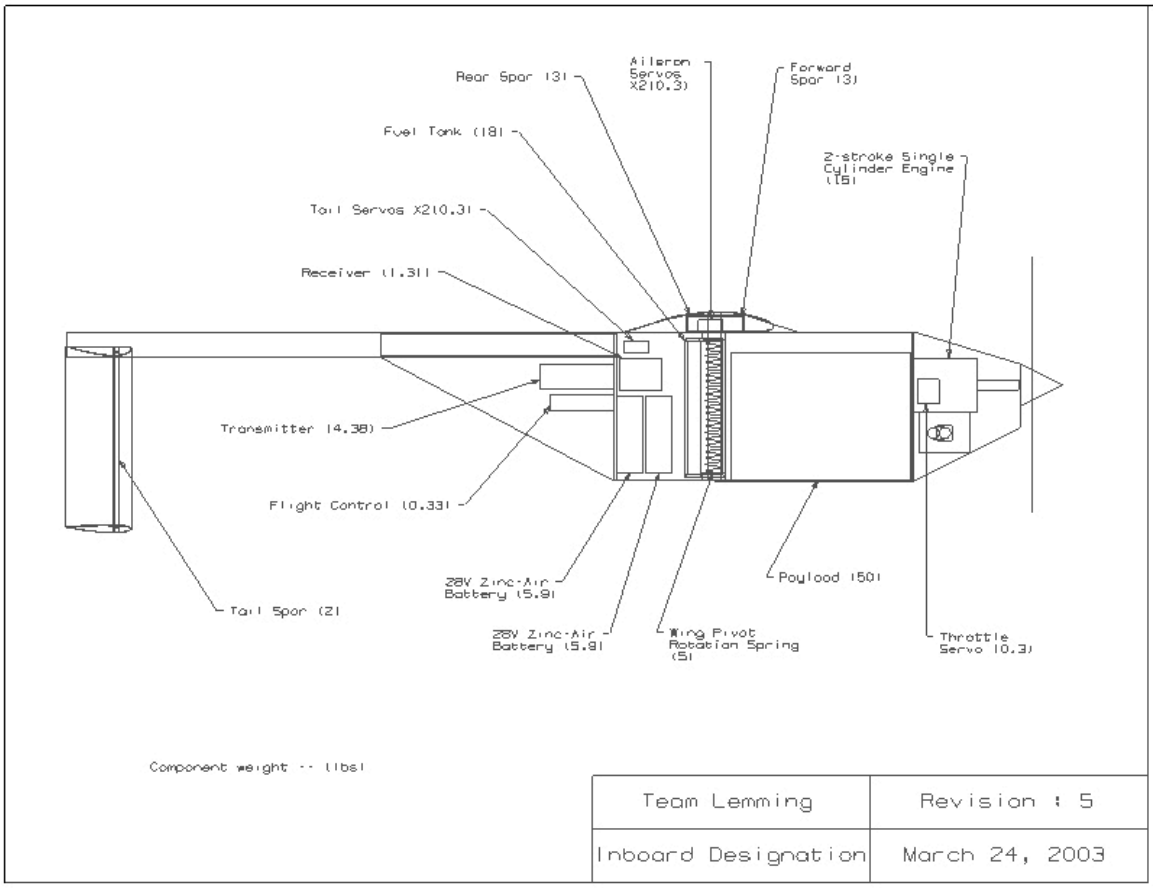

Figure 14.5: Location of CUAV systems.

14.6 Deployment Systems

14.6.1 Boom Deployment

This method of deployment will entail the use of a dedicated structure fixed inside the transport craft. This structure will act to support the UAV and extend it out of the cargo bay for release into flight. The UAV will simply be released from the boom to drop and begin its mission. The boom will extend the UAV well into the free stream flow away from any part of the transport craft. Having the UAV isolated during release eliminates any problems or risks associated with store separation and collision between the two craft. The UAV wing will be folded while the UAV is stored within the transport as well as during the extension of the boom. Prior to release, the wing will be unfolded and the engine started. The UAV is supported on the boom in two places (fig 14.6). The main attachment is through the wing pivot to allow the wing to rotate while attached to the boom. A secondary attachment is located at the end of the boom. This attachment acts to stabilize the UAV while on the boom and constrain its motion.

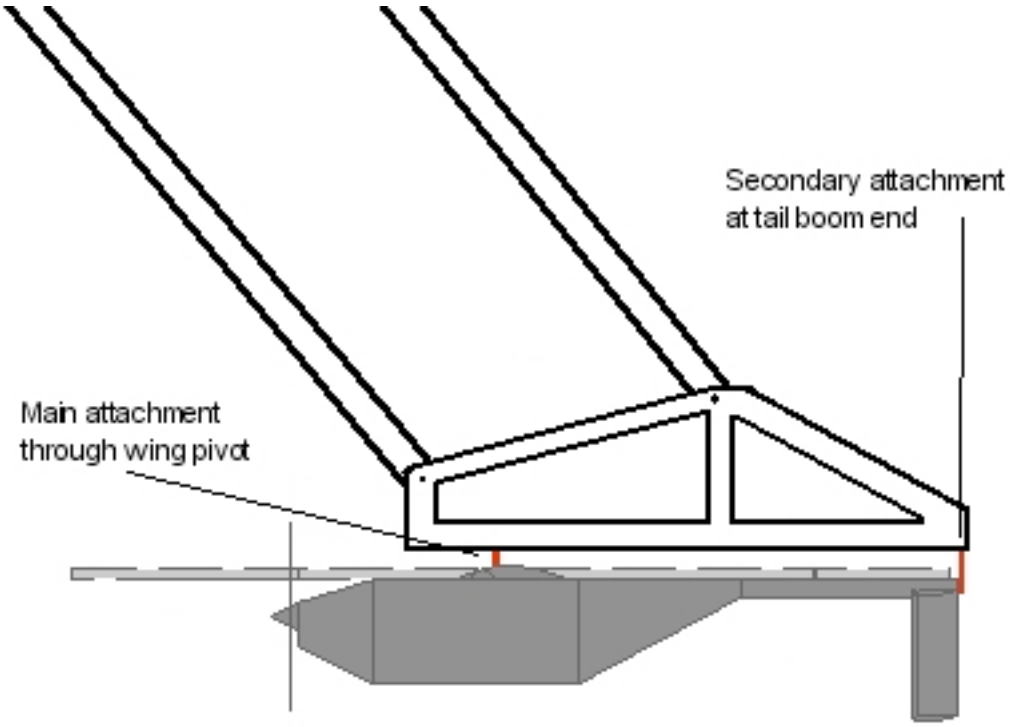

Figure 14.6: UAV boom in extended position

The boom system will be composed of a system of aluminum trusses. The entire structure will be attached to a track system within the transport to allow the boom to extend out as well as down. A hydraulic system will likely be used to actuate the boom.

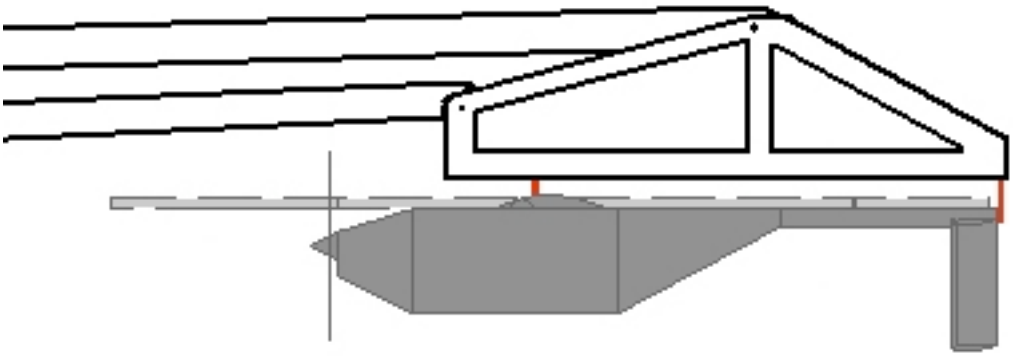

Figure 14.7: UAV boom in stored position

14.6.2 Towline Deployment

One type of deployment being incorporated into the UAV is the tow line deployment method. This will be accomplished by attaching a small ring to the nose cone of the UAV and using a two hundred foot long tow rope to connect the UAV to the towing aircraft. This length was determined based on

researching suggested towline lengths online. Some testing of different lengths with a full-sized prototype will be required to find the minimum length the towline can be. The Birren Linknife system will be used to cut the rope when the UAV is ready to be deployed. Figure 14.8 shows the Linknife system.

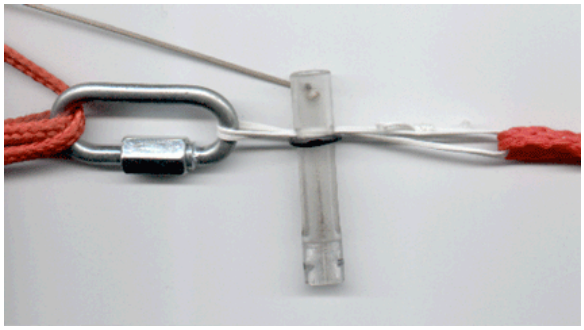

Figure 14.8: Birren Linknife system.

14.6.3 Parachute Deployment

For the drag chute deployment method a parachute would be attached to the end of the tail-boom of the UAV. This parachute would be used to both extract the UAV from the transport aircraft, and to slow the UAV down. Sizing for the parachute was done for a terminal velocity of 200ft/sec and at 10,000ft altitude. A drag coefficient of 1.2 was used for the parachute, accounting for a lower drag in a parachute than a hollow hemisphere, which has a drag coefficient of 1.42. Using these numbers the parachute was sized to have a diameter of 2.3 feet.

Chapter 15 Cost Analysis

15.1 Cost Overview

As with all aircraft, estimation of the cost of the CUAV was a critical part of the design process. Since the CUAV was designed as an expendable aircraft, the cost must be kept low to make the Lemming UAV a preferable choice over existing reusable UAV systems. The following sections describe how the team arrived at the estimated affordable price for the CUAV.

From a cost standpoint, the team is solely concerned with the fly-away cost of each vehicle. Operational costs such as maintenance, support, upgrades, and disposal are not relevant to the CUAV due to the expendable nature of its mission. Therefore, the cost analysis of the CUAV considers only the

following costs: conceptual engineering design, detailed design, airframe manufacturing, systems acquisition, UAV assembly, flight test and evaluation engineering.

15.2 Engineering Costs

To estimate engineering costs, the group assumed that our seven member team could perform all engineering analysis and design necessary for the construction, testing, and certification of the production aircraft. The analysis allows the team 3 months to perform initial concept evaluation. 3 additional months are allotted for detailed design of the craft leading up to the production and assembly of the UAV. Following completion of the first units, the team allows 3 more months of engineering analysis to perform flight test evaluations on the design and make any necessary alterations before full scale production. This comes to a total of 9 months of product engineering with a seven person team. It is assumed that each team member is being paid a salary of $ 25 per hour.

Summing up these numbers results in an estimated product engineering cost of $ 252,000. To allow for unforeseen difficulties in the design, this number was rounded up to 300,000 total engineering costs for the project. For a projected initial order of 200 units, these engineering costs come to $ 1,500 per unit.

15.3 Airframe Cost

Estimation of the cost of the UAV airframe proved to be the more difficult part of the cost analysis. The unique aerial deployment aspect of the CUAV mission required a custom built airframe incorporating a swing-wing system. This precluded the use of existing airframes. Therefore, the only way to truly know the cost of the airframe would be to submit plans to manufacturers and ask for bids on the project. With no project funding and no immediate plans to produce the aircraft, it was determined that manufacturers would not be willing to commit engineering resources into creating a bid for the CUAV airframe contract. Consequently, Team Lemming was forced to estimate the cost of the CUAV airframe from historical data.

The team decided that a good way of finding the cost of an airframe is by finding the cost for homebuilt kits. One problem the team ran into during this search is that not all kits are made from one

material type. For example, many composite kits use metal, and wood in them, like the Rand Robinson KR-1 and KR-2. Since the most basic definition of a composite is not limited to laminated cloth and foam materials, the team decided to list these kits simply as composites. Another break down in the kit definition was whether the kit came from a supplier like Aircraft Spruce, or Wick's Aircraft Supplies, or if the kit came from the designer and manufacturer, such as New Glasair LLC, or Sonex Ltd.

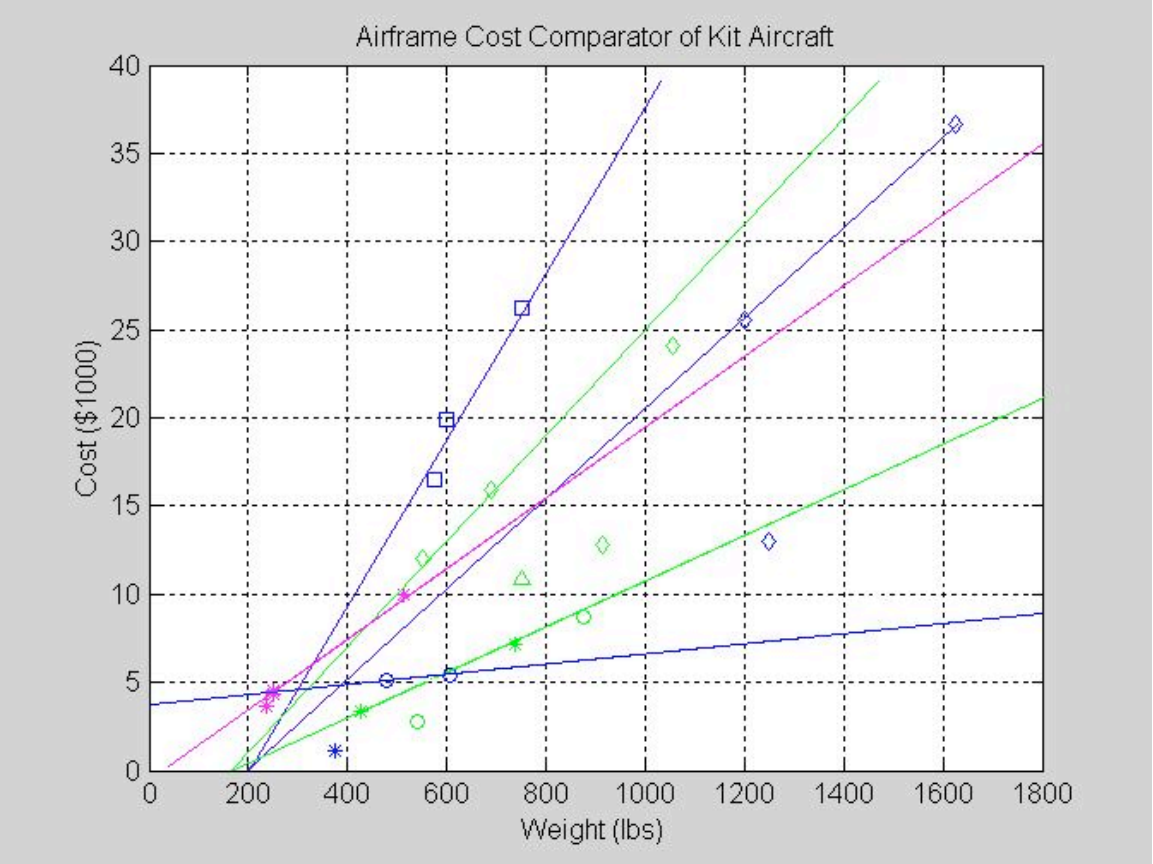

Figure 15.1: Cost data on kit-planes used to estimate materials costs for CUAV airframe.

The data was compiled and plotted on a graph (Figure 15.1) along with trend lines to distinguish the data sets. Once the data was compiled it was also found that Glasair and Glastar composite manufactured kits had a different cost to weight ratio than other composite kits produced my manufacturers. These manufactured kits were grouped on their own because of this. These trend lines showed that the maximum cost of the airframe material would be approximately $4,000 based on the 2 place, Composite kits from a supplier data line. The team assumed that with an order of 200 units and competitive bidding, and realizing that the CUAV is much smaller than the homebuilt craft analyzed, the

airframe materials could be acquired for $ 3,000. The team then allowed $2,000 for labor to assemble the airframe. This brings the assembled airframe cost up to $ 5,000.

15.4 Systems Cost

Great care was taken in the choice of the systems used in the CUAV to control the cost of the craft. System decisions were based chiefly on unit cost. Therefore, the cost of each system component used in the design is known. Table 15.1 shows the breakdown of the systems cost. As shown in the table, the total cost for the UAV systems is $ 18,000.

Table 15.1: CUAV systems costs

Systems Cost	
System	**Cost per Unit**
Data Link	$15,000
Autopilot / Navigation	$2,000
Servos	$ 70 x 6
Batteries	$580
Total	$18,000

15.5 Assembly Cost

The final cost included is the actual assembly of the UAV components. This includes the assembly of the airframe components as well as mounting and integrating the internal systems. Following assembly, each unit would have to be inspected to verify that the systems are functioning properly and that the assembly was performed correctly. The group estimates that a total of 32 man-hours per unit would be required for assembly, testing, and quality assurance. At $20 per hour, this comes to a cost of $640 per unit.

Table 15.2: UAV cost summary.

UAV Cost Summary per Unit	
Product Engineering	$1,500
Airframe	$5,000
Systems	$18,000
Assembly / Testing	$640
Total Cost	**$25,140**

15.6 Cost Summary

Summing the costs listed in the preceding sections results in the fly-away production cost for the CUAV. Table 15.2 shows the estimated total cost. As shown in the table, the estimated production cost for the CUAV excluding payload is $25,140. It should be noted that this price does not include a profit margin and is for the air vehicle only and therefore does not include the payload.

Chapter 16 Conclusion

The Team Lemming CUAV is the cheapest available reconnaissance UAV design available to the U.S. Navy. Clarifying and defining the driving factors of the Navy supplied RFP were the first actions performed by the team. This lead the team to find all the UAVs in production, to see if any fit the RFP. The team discovered that no UAVs could be aerial launched, and the most of them were too expansive to be considered expendable. The team used the RFP to evaluate the varied initial designs, as well as deployment methods. This evaluation led to the selection of three preferred concepts. The preferred concept's initial size was optimized, and analyzed to provide the minimum manufacturing cost with the highest deployment success rate. The lemming team finally found that a Scissor Wing concept could be manufactured to fit the different deployment types while still fulfilling all of the RFP requirements, especially the minimization of cost.

The Team Lemming CUAV has several interesting features which make it such an economical aircraft to build and purchase. These features tend to fall in 2 categories: Design for ease of manufacture, Utilization of cheap systems parts. The design for ease of manufacture can be seen in several places. The fuselage is composed of flat rectangular and triangular pieces of laminated Kevlar. This means that large flat sheets of Kevlar can be cured like Plywood and the cut to the desired shape just as readily. The CUAV has several aspects that reduce cost manufacturing. The wing has is straight tapered with no twist, allowing it foam core to be quickly and simple cut with a hotwire. The airfoil's flat bottom allows for a simple installation onto the fuselage, and also makes covering and sanding the core's composite skin easier. Using the same front and rear spar allows for a reduction in parts, and there for cost.

The small size of the Team Lemming CUAV allows for some innovative approaches to systems design. The team can use RC _ scale electric servos to actuate the control surfaces, which are significantly cheaper than their commercial aviation counterparts. The stable design of the CUAV allows the team to utilize an autopilot also originally designed for RC aircraft. Finally, the team has used communications systems already developed and in production for the Shadow 200. Thus the manufacturers would be buying a proven and cheap communications system. The systems components selected show that the destruction or capture of the aircraft would not result in a major cession of technology to an enemy.

This is the Team Lemming response to the NAVY Request For Proposal for a minimum cost UAV deployable from an aircraft. This aircraft has been designed to be cheaper than any other UAV currently available, while still fulfilling or exceeding all of the RFP requirements. The Lemming CUAV is the best design for a cheap UAV because of its systems selection and ease of assembly.

References

2.1 Jane's Aircraft Journal 1999-2000 pgs 522-524, 636-637, 676

2.2 Jane's Aircraft Journal 1993-1994, pg 502.

2.3 Jane's Aircraft Journal 1988-1989, pg 394

2.4 Boeing Company "V-22 Osprey", http://www.boeing.com/rotorcraft/military/v22/flash.html, 2002

2.5 "US Military Aircraft," http://www.fas.org/man/dod-101/sys/ac/index.html, 2002

2.6 Pioneer UAV, Inc. "Pioneer: The System", http://www.puav.com/pioneer_specifications.asp, 2002

2.7 Aftergood, Steve. "Pioneer Short Range (SR) UAV", http://www.fas.org/irp/program/collect/pioneer.htm, March 5, 2000

2.8 Lee, Jeff, and Purdy, Carol. "NASA GSFC/Wallops Flight Facility: Unmanned Aerial Vehichles: SASS Lite," http://uav.wff.nasa.gov/db/uav_char.html?key=21

2.9 Mullowney, Pete, "(Shadow) 200," http://www.aaicorp.com/defense/uav/200.html, AAI Corporation, 2002

2.10 Lee, Jeff, and Purdy, Carol. "NASA GSFC/Wallops Flight Facility: Unmanned Aerial Vehichles: Shadow 200," http://uav.wff.nasa.gov/db/uav_char.html?key=23

2.11 Mullowney, Pete, "(Shadow) 400," http://www.aaicorp.com/defense/uav/400.html, AAI Corporation, 2002

2.12 UAV Forum, "UAV Forum | Vehicles | Production | Sentry," http://www.uavforum.com/vehicles/production/sentry.htm

2.13 UAV Forum, "UAV Forum | Vehicles | Developmental | Shadow 200," http://www.uavforum.com/vehicles/developmental/shadow200.htm

2.14 UAV Forum, "UAV Forum | Vendors | UAV Systems | AAI," http://www.uavforum.com/vendors/systems/aai.htm , 2002

2.15 Lee, Jeff, and Purdy, Carol. "NASA GSFC/Wallops Flight Facility: Unmanned Aerial Vehichles: Freewing," http://uav.wff.nasa.gov/db/uav_char.html?key=40

2.16 Freewing Aerial Robotics Corp, "Products: Scorpion 100-50," http://www.freewing.com/scorpion100-50.html , 2002

2.17 Lee, Jeff, and Purdy, Carol. "NASA GSFC/Wallops Flight Facility: Unmanned Aerial Vehichles: Huntair," http://uav.wff.nasa.gov/db/uav_char.html?key=11

2.18 Lee, Jeff, and Purdy, Carol. "NASA GSFC/Wallops Flight Facility: Unmanned Aerial Vehichles: Porter," http://uav.wff.nasa.gov/db/uav_char.html?key=17

2.19 Lee, Jeff, and Purdy, Carol. "NASA GSFC/Wallops Flight Facility: Unmanned Aerial Vehichles: Truck," http://uav.wff.nasa.gov/db/uav_char.html?key=31

2.20 FAS Webmaster, "AGM-136 Tacit Rainbow," http://www.fas.org/man/dod-101/sys/smart/agm-136.htm , December 31, 1998

2.21 Voth, Peter, "AGM-142 Raptor / Have Nap / Popeye – Smart Weapons," http://www.fas.org/man/dod-101/sys/smart/agm-142.htm , December 20, 2001

2.22 FAS Webmaster, "AGM-154A Joint Standoff Weapon [JSOW] – Smart Weapons," http://www.fas.org/man/dod-101/sys/smart/agm-154.htm , June 27, 2000

2.23 FAS Webmaster, "AGM-158 Joint Air to Surface Standoff Missile (JASSM) – Smart Weapons," http://www.fas.org/man/dod-101/sys/smart/jassm.htm , September 18, 2002

2.24 FAS Webmaster, "Tri-Service Standoff Attack Missle TSSAM – Smart Weapons," http://www.fas.org/man/dod-101/sys/smart/tssam.htm , February 19, 1998

2.25 O'neill, J. P., "AGM-86B/C Factsheet," http://www.af.mil/news/factsheets/AGM_86B_C_Missiles.html

2.26 FAS Webmaster. "AGM-86 Air-Launched Cruise Missle [ALCM] United States Nuclear Forces," http://www.fas.org/nuke/guide/usa/bomber/alcm.htm, August 14, 2000. Including picture: us_agm86b_01.jpg

2.27 Clinard, Tom. "The B-52 and its Missiles," http://www.ammsalumni.com/B52missiles.html, January 28, 2002

2.28 Sublette, Carey. "The W-80 Warhead," http://nuketesting.enviroweb.org/hew/Usa/Weapons/W80.html, September 1, 2001

2.29 FAS Webmaster. "B-52 Stratofortress," http://www.fas.org/nuke/guide/usa/bomber/b-52.htm, April 23, 2000.

4.1 Raymer, Daniel P. *Aircraft Design: A Conceptual Approach.* AIAA, Reston, VA, 1999.

4.2 Mason, W.H, computer program "Acsize", Aircraft Design Software Bundle.

4.3 Team Lemming, *Low-cost Expendable UAV Fall Semester Report,* Virginia Tech, 2002.

4.4 Mason, W.H, Fortran program "friction.f", www.aoe.bt.edu/ao/faculty/Mason f/friction.f. 1989.

6.1 Team Lemming, *Low Cost Expendable UAV, Fall Semester Report,* Virginia Tech, 2002.
6.2 Daniel P. Raymer, *Aircraft Design: A Conceptual Approach,* AIAA, 1999.
6.3 Marie Radne, email communication, 24 February 2003.
8.1 Raymer, Daniel P., *Aircraft Design: A Conceptual Approach,* AIAA, 1999.
9.1 Mason, W.H, Fortran program "friction.f", www.aoe.bt.edu/ao/faculty/Mason f/friction.f. 1989.
9.2 Mason, W.H., "Experiment 7 – Aero/Hydrodynamic Testing," April 5, 2002, http://www.aoe.vt.edu/~devenpor/aoe3054/manual/expt7/text.html

9.3 Abbot, I.A., and Von Doenhoff, A.E., *Theory of Wing Sections,* 1959, Dover Publications, Inc., New York, N.Y., pg. 489.

9.4 Bertin, J.J., and Smith, M.L., *Aerodynamics for Engineers, Third Edition,*1998 Prentice-Hall, Inc., Upper Saddle River, N.J., pp. 40.

9.5 Digital Dutch, "1976 Standard Atmosphere Calculator," 2003, http://www.digitaldutch.com/atmoscalc/index.htm

9.6 Selig, M., "UIUC Airfoil Coordinates Database," December 6, 2002, http://www.aae.uiuc.edu/m-selig/ads/coord_database.html

12.1 Megson, T.H.G. Aircraft Structures for Engineering Students
John Wiley & Sons Inc., New York 1999

12.2 http://adg.stanford.edu/aa241/structures/vn.html

12.3 Beer, Ferdinand and Russel Johnston jr. Mechanics of Materials
McGraw-Hill Inc., New York 1992

12.4 Mangonon, Pat The Principles of Materials Selection for Engineering Design
Prentice Hall, New Jersey 1999

14.1 Susan Opp, *L-3 Communications,* email correspondence, 22 February 2003.

14.2 Bruce Hobbs, *AACOM Systems,* email correspondence, 18 March 2003.

14.3 *Micropilot Products,* Micropilot Inc., available at : http://www.aerospaceweb.org/aircraft/fighter/f15/index.shtml, accessed 2003.

14.4 Larry Dungan, *Nicad Knowledge,* High Flight Ariticels, available at: http://www.fly-imaa.org/imaa/hfarticles/electro/v11-4-44.html, accessed 2003.

14.5 Tim Resler, *Radio-Recon,* email correspondence, 20 February, 2003.

14.6 Mike Bennis, *Electric Fuel Corp.,* email correspondence, 20 February 2003.